UNIVERSITY OF ALGARVE

Faculty of Science and Technology

BEACH VOLUMETRIC ANALYSIS AND WAVE FORCING ALONG AN IRISH BEACH SYSTEM

Geomatic Master, specialization in Geographic Information Science

ANA LUÍSA BANJA MARTINS

Work made under the supervision of Professor Óscar Ferreira

and Professor Derek Jackson

FARO

2014

UNIVERSITY OF ALGARVE

Faculty of Science and Technology

BEACH VOLUMETRIC ANALYSIS AND WAVE FORCING ALONG AN IRISH BEACH SYSTEM

Geomatic Master, specialization in Geographic Information Science

ANA LUÍSA BANJA MARTINS

Dissertation submitted to obtain the Master degree in the Geomatic Master Course, awarded by The Faculty of Science and Technology and The High Institute of Engineering, University of Algarve.

SUPERVISORS

Professor Óscar Ferreira

Professor Derek Jackson

FARO

2014

BEACH VOLUMETRIC ANALYSIS AND WAVE FORCING ALONG AN IRISH BEACH SYSTEM

Work authorship statement

I declare to be the author of this work, which is unique and unprecedented. Authors and works consulted are properly cited in the text and are included in the listing of references included.

The candidate

_____

Ana Luísa Martins

Faro, …..…/…..…/…..…

ACKNOWLEDGMENT

This project lasted about two years and during its development I received the support of several people, to whom I express here my sincere thanks.

My first words go to Professor and Supervisor Óscar Ferreira, who encouraged me in choosing this theme, for his support, attention, availability, sharing of knowledge and suggestions transmitted throughout this journey and making this work much more attractive.

Also, my thanks go to my Supervisor Derek Jackson, for his crucial support in my experience abroad. The sharing of knowledge and ideas were undoubtedly of great importance.

To my colleagues Carlos Loureiro and Mara Nunes, for their support and invaluable contribution to the success of this Dissertation.

To my "aunt" Lorraine, for all the time invested in correcting the writing of this Dissertation.

To my friends, although few they were sufficient to make me feel happy and supported.

Special words go to my family, for their caring and patience, and as always, for being present at another important step in my life.

BEACH VOLUMETRIC ANALYSIS AND WAVE FORCING ALONG AN IRISH BEACH SYSTEM

Abstract

Five Finger Strand, a bedrock-framed beach located between Five Finger rock and the mouth of Trawbreaga Bay, Republic of Ireland, appears to experience high temporal and spatial variability in erosion and accretion because the coast is forced by multiple mechanisms that operate over different time scales (Cooper et al., 2007). To identify all states the beach can present, their frequency of occurrence and dynamics, it the study of beach profiles was implemented in which beach volumetric analysis was used to determine and predict beach evolution. Additionally incident waves were analysed and statistical analysis applied on these.

Owing to data complexity, a Geographic Information System (GIS) tool – BeachPROG – was developed to facilitate data analysis. As input it uses Differential Global Positioning System (DGPS) data and outputs Digital Elevation Models (DEMs), beach volumes, profiles and respective areas and slopes, through *Python* script. In general, this tool revealed good results, as the data automation, visualisation, spatial consultation, and spatial analysis can be accessed in a much more intuitive way than through existing methods. Equally, this tool can serve as a methodological base for other investigations, presenting a fully commented, easy script structure that enables further modifications and/or script accretions.

Data from the BeachPROG tool, were compared against hydrodynamic data at the site. The existence of variations in beach behaviour caused by wave forcing was clearly evident. However, in some cases it was equally possible to verify that even being exposed to conditions capable of causing significant changes, the beach remained stable.

A deep knowledge on how waves and inlet dynamics interact with the beach, changing its behaviour, was however, not the main aim of this thesis, since the main goal was to develop and test the GIS based tool. Previous studies analysing similar forcing agents

showed different beach behaviours, for the study area, indicating that further and more detailed studies must be performed.

Key-words: Beach profile, beach volume, GIS tool.

ANÁLISE VOLUMÉTRICA DE PRAIA E ATUAÇÃO DAS ONDAS AO LONGO DE UM SISTEMA DE PRAIAS DA COSTA IRLANDESA

Resumo

A praia Five Finger Strand, de estrutura rochosa e compreendida entre a rocha Five Finger e a barra de maré do Trawbreaga (M. C. O' Connor, Cooper, & McKenna, 2009), República da Irlanda, evidencia ser condicionada por diversos mecanismos, causando variabilidade sedimentar temporal e espacial (Cooper et al., 2007). Para a correta identificação dos comportamentos que a praia pode apresentar, respetiva frequência e dinâmica com que ocorrem, foi implementado o estudo de perfis de praia, tendo-se recorrido às análises volumétricas para determinar a sua evolução. Adicionalmente, estudou-se a atuação das ondas incidentes e implementou-se uma análise estatística.

Devido à complexidade dos dados, foi desenvolvida a ferramenta SIG – BeachPROG – para facilitar o tratamento de dados. Esta ferramenta usa dados DGPS para originar MDEs, perfis de praia, volumes e respetivas áreas, através de códigos em *Python*. No geral, esta ferramenta revelou estar apta a desenvolver as tarefas definidas, sendo que a automatização dos dados, visualização, consulta e análise espacial podem ser executadas de forma bastante intuitiva. A ferramenta está igualmente apta a servir como base metodológica para outras investigações, apresentando um código totalmente comentado e de fácil estrutura, permitindo assim futuras modificações.

Após obtenção dos dados com a ferramenta BeachPROG, foram realizadas comparações com dados da agitação marítima. A existência de variações comportamentais da praia causadas por alterações na atuação das ondas foi bastante evidente. No entanto, em alguns casos foi igualmente possível verificar que, mesmo existindo todas as condições capazes de provocar alterações significativas na praia, esta manteve-se estável.

Não foi possível, nesta dissertação, saber em detalhe como estes dois mecanismos atuam na praia e qual o agente predominante para cada condição, visto que o objetivo principal foi o desenvolvimento e teste da ferramenta. Estudos anteriores revelaram que, para condições hidrodinâmicas semelhantes, diferentes comportamentos da praia foram obtidos, reforçando a necessidade da realização de estudos mais detalhados.

Palavras-chave: Perfil de praia, volume de praia, ferramenta SIG.

INDEX

FIGURE INDEX

TABLE INDEX

ABBREVIATIONS

Symbols:

≈	Approximately equal to
ρ	Correlation
°	Degree
δ	Dirac delta function
≤	Less than or equal to
-	Minus
%	Percent
+	Plus
±	Plus-minus
Σ	Summation
®	Registered trademark

Abbreviations:

X, Y, Z	Cartesian Coordinate System.
CIAT	Coastal Impact Assessment Tool.
DGPS	Differential Global Positioning System.
DEM	Digital Elevation Model.
DRG	Digital Rater Graphics.
DSAS	Digital Shoreline Analysis System.
ESRI	Environmental Systems Research Institute.
ECMWF	European Centre for Medium-Range Weather Forecasts.
GIS	Geographic Information System.

GUI	Graphical User Interface
Hso	Wave Height
SN	Inspection Density.
LIDAR	Light Detection And Ranging.
ME	Mean Error.
Mwd	Mean wave direction.
Mwp	Mean wave period.
NAO	North Atlantic Oscillation.
PDF	Portable Document Format.
RBF	Radial Basis Functions.
RMSE	Root Mean Square Error.
Swh	Significant Wave Height.
S	Standard Deviation.
TXT	Text.
VBA	Visual Basic for Applications.
WAM	Wave Modelling.

Mathematical units:

cm	Centimeter.
m^3	**C**ubic meters.
km	Kilometer.
m	Meter.

mm	Millimeter.
s	Seconds.
cm^2	Square centimeter

Wind Rose:

S	South
SSW	South-southwest
SW	South-west
SWS	Southwest by south
W	West
WNW	West-northwest
N	North

CHAPTER 1

1 INTRODUCTION

1.1 DISSERTATION SUBJECT

The Dissertation "Beach Volumetric Analysis and Wave Forcing along an Irish Beach System" is part of the Geomatic Master, specialisation in Geographic Information Science.

A user-friendly GIS tool was developed that enables the quantification of volumetric changes. The tool was applied to the beach of Five Finger Strand (Republic of Ireland), analysing large-scale coastal measurements, and also the correlation link between results from developed GIS tool and sea waves dynamics.

This investigation was held between the University of Algarve (Portugal) and University of Ulster (Northern Ireland).

1.2 RATIONALE OF THE STUDY TOPIC

Human population growth and its associated developments are placing enormous pressure on coastal resources and are requiring effective environmental planning, conservation and protection as a result. The knowledge of economic and environmental impacts requires an understanding of the way that terrestrial and marine processes operate and interact in the coastal zone (Morton, 1979).

Coastal environments often appear to experience high temporal variability in erosion and accretion because the drivers of coastal change are forced by multiple mechanisms that operate over a large range of time scales including: wave swash and backwash (seconds–minutes), tides (hours–months), climate and changes in storm amplitude and frequency

(years–decades) and relative sea-level rise (centuries–millennia) (Larson et al., 1999). A number of researchers state that beach mobility is also a function of the geological framework (Klein and Menezes, 2001; Jackson and Cooper, 2009 and Jackson et al., 2005), such as the distance between headlands, bay shape, grain size and nearshore slope. Moreover, additional influence on environments adjacent to tidal inlets arise from changes in channel dimensions and position, reconfiguration of tidal deltas, changing tidal prism, as well as interaction with other channels (O'Connor, et al., 2011).

To acquire a deep knowledge of beach morphology it is essential to identify all different states a beach presents and their frequency of occurrence. Equally important is the understanding of beach dynamics, which require the identification of physical mechanisms involved in the beach shape modification (Sénéchal et al., 2009).

The behavioural knowledge of coastal environments is limited by the time scale of measurements. On the time scale of hours to months measurements are taken generally to relate hydrodynamic processes to sand movement and beach morphology changes (eg., Anfuso, 2005; Masselink et al., 2007). Over longer intervals ranging from months to years, our understanding of beach erosion dynamics during a certain time period is very difficult to quantify because high-frequency surveys are not typically sustainable and measurement accuracy degrades severely as sampling frequency decreases. For example, seasonal or yearly beach profile measurements will not capture details of storm-induced erosion and subsequent beach accretion that occurred in the middle of the sampling year. In contrast, at intermediate time scales beach erosion and accretion are commonly derived from time series of shore-normal elevation profiles and changes in the position of the shoreline (Farris & List, 2007). However, even comparing pre- and post-storm beach surveys, spaced only a few days apart, there is an under-predict of results because beach recovery typically begins *immediately* after a storm event (List et al. 2006; Zhangand Whitman, 2007).

As the beach is exposed to a variety of external processes, constantly changing its shape, the study of beach profiles over the long term seems to be the best way to predict coastal behaviour according to changes on wave and tidal conditions. A beach profile represents the cross-shore morphology of the beach along the coast and it may extend out through the offshore region to beyond the dunes (Kaiser & Frihy, 2009). The response of beach

profiles to changing hydrodynamic conditions is related to the equilibrium beach profile concept, wherein is dependent on numerous factors such as grain size (Dean, 1991), changes on sea level or on sediment supply (Storms et al., 2002), incidence of storms, beach state (Carter and Balsillie, 1983) among others.

Different approaches are cited in the literature to predict variations in beach profiles such as process based mathematical and numerical models, deterministic process based models, probabilistic models, wave let models, inverse models and data-based models (Hashemi et al., 2010). Beach volumetric analysis is one of the most commonly used approaches to determine variations in beach profiles and afterward to predict beach evolution. Forecasts can even be made by fitting deterministic trends through the data and extrapolating them into the future (Southgate, 2008). For that purpose, sufficiently long and accurate time series of beach volumes measurement, characterised by specific spatial coverage, spatial resolution, temporal resolution, and overall length in time (Kroon et al., 2008), must be collected using traditional survey techniques, video imagery, remote sensing DGPS or terrestrial laser (scan).

Studies applying beach profiles analysis are relatively common in literature with distinct approaches according to field sites and measurement techniques. Li et al. (2005); Kabdas & Tu (2006); Kaiser & Frihy, (2009); Hashemi et al., (2010) and Muñoz-Perez & Medina, (2010) are some examples of this variety.

Beach profiling has also been extensively used in Northern Ireland, in studies focused on the identification of external forcing factors and quantification of their contribution to coastal behaviour, such as Cooper et al. (2004, 2007); Jackson et al. (2005); O'Connor, et al (2007, 2011).

The procedure for understanding and predicting beach volume changes consists primarily of analysing hydrodynamic forcing (waves, currents, water levels) and then applying a correlation or a statistical analysis derived from an explicit comparison of the beach volume and hydrodynamic data series (Southgate, 2008). Because of the complexity of the system, the data obtained from any of these sources needs to be manipulated in order to analyse spatial characteristics and to represent them graphically. The advent of GIS technology has facilitated such analysis (Andrews *et al*., 2002). GIS has provided new

spatial analysis and data integration techniques for accurate mapping and analysis of many dynamic coastal environments. GIS for coastal research purposes also enables a simplified data access, easy data editing and updating, and on-the-fly visualisation of coastal hazards (Bossak *et al*., 2005).

Despite the advances made with GIS software, the extensive period between the introduction of raw data in the system and the final result makes the work difficult and slow. This led to the construction of GIS tools, as versatile and flexible as possible, that on the one hand enable the data automation, visualization, spatial consultation, spatial analysis, and geostatistical analysis in a much more intuitive way (Rodríguez, et al., 2009), and on the other hand allow the access of final results with reduced time consumption.

1.3 METHODOLOGY IMPLEMENTED

The main goal of this dissertation is the construction of a GIS tool to analyse beach surveys/profiles. This need arises from the data accumulation of field studies of the scientific group at the University of Ulster. The field work on the Five Finger Strand (and other beaches) was conducted over several years in order to relate the morphodynamics of the beach with the action of external factors.

The methodology discussed in this Dissertation is separated into two distinct parts:

1. The creation of a GIS tool. This tool allows the input of DGPS data and the output of DEM, beach volumes, profiles and respective areas, volumes and slopes. This tool was created specifically for beach profile surveys, in order to enable a more rapid and convenient extraction of results. The output data can then be stored and used for coastal dynamic analysis;
2. Study of the relation between forcing factors and data obtained from the GIS tool. In order to study the coastal dynamics of Five Finger Strand, sea waves data were used to relate medium and maximum wave height between periods with the volume changes obtained by the GIS Tool to understand if the observed variations can be correlated directly with wave height variations. Other parameters such as

the sea wave direction and lateral sediment transport were also used to determine the influence of storms on coastal morphodynamics.

1.4 DISSERTATION STRUCTURE

The present work is divided into chapters, each one with a specific approach to the study phase (Figure 1.1).

In the second chapter a description is given of the state-of-the-art on the topic, which addresses the issues related to the morphodynamics of beaches and the action of forcing agents, such as marine action and the occurrence of storms, as well as the potential use of GIS tools for the analysis of coastal processes. Also considered in this chapter are advances of studies related to beach morphodynamics and studies conducted in the same study area.

A more detailed approach of the study area is presented in the third chapter, including a description of the morphodynamic and hydrodynamic aspects of the region.

The fourth chapter describes the methodology used to achieve the objectives set for this study. It is possible to find in this chapter a description of the fieldwork that has been used for collecting geographic information from the beach in study, the pre-processing of data, the development of the GIS tool, a guide use of the tool and the quantitative analysis resulting from the comparison between morphological and environmental factors.

The fifth chapter describes results obtained within this Dissertation and consecutively, the sixth chapter discusses the application of the developed tool for the study area, the comparison of the results arising from the tool with the forcing factors and an examination of the applicability of the developed tool.

Finally, in the last chapter, the concluding remarks obtained with this research are presented.

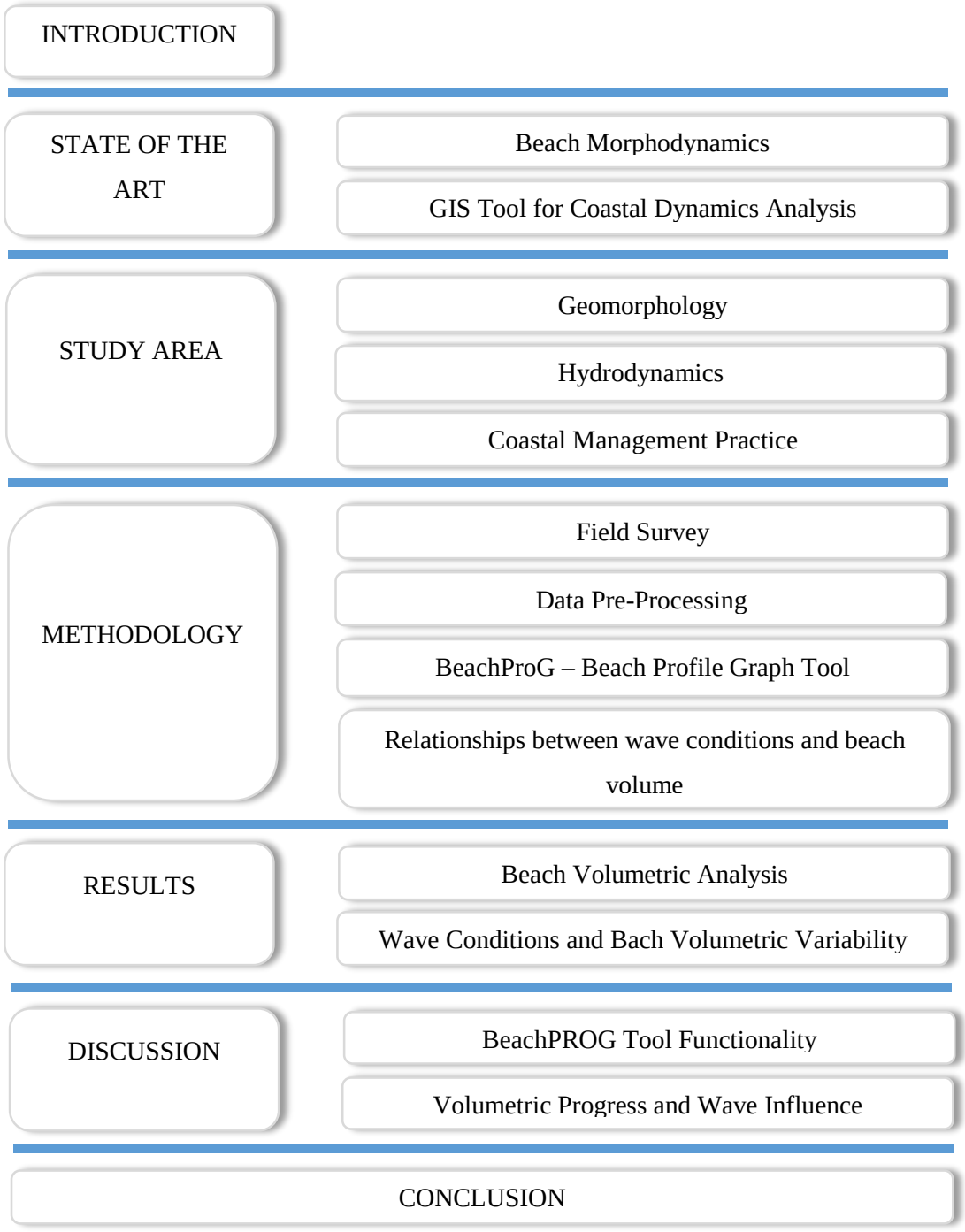

Figure 1.1: Dissertation structure.

CHAPTER 2

2 STATE OF THE ART

2.1 BEACH MORPHODYNAMICS

Beaches are naturally highly dynamic and their behaviour is often complex and difficult to study. The intertidal zone, loosely defined as the transition area between the dry beach and the nearshore, is a friction-dominated area where sediment redistribution depends on geological controls (bedrock geology, accommodation space, sediment volume, etc.), sedimentary factors (grain shape, packing, composition, porosity, lithification, drainage, biological activity, etc.), as well as dynamic factors (secondary wave motions, tidal currents, edge waves, upwelling/downwelling, gravity, etc.) (Cooper & Pilkey, 2004). Additionally at beaches adjacent to tidal inlets, other influences such as interaction with nearby channels, their changes on position and dimensions, reconfiguration of tidal deltas, and changes on tidal prisms (Morton et al., 2007 and Cooper et al., 2007) determine beaches' behaviour.

Despite the wide acceptance of the influence of the factors described above, there is no unanimity in regard to these factors importance. For many, waves and tides are the foremost factors that contribute to the coastal morphodynamics (Davis & Hayes, 1984). In this case, beaches dominated by the influence of waves are called wave-dominated coasts and those dominated by tides are called tide-dominated coasts. The beach may exhibit tide-controlled morphology when wave energy is low to nil. This state may become dispersed by waves during the high-energy season, resulting in a profile that reflects mixed domination. Generally, the larger the tidal range, the more important the intertidal volume of sand or gravel, and the higher the wave energy levels required in order for large-scale morphological changes to occur. As a result, the rates of sediment transport and beach morphological change are retarded on beaches with large tidal ranges

and lower modal wave energy. As tidal action increases, the shallow shoreface and inner shelf topography may be characterised by numerous banks and ridges that are typical of a tide-dominated process signature. Levoy et al. (2000) also verified that the larger the tidal range, the greater the variations in morphodynamic behaviour between the lower beach and the upper beach. Mixed coasts would be expected to show stable large-scale morphological and sedimentary patterns that are quite distinct from those of pure wave-dominated and tide-dominated coasts (Anthony & Orford, 2002).

As well as waves and tides, the effect of winds can also affect the coastal morphology both directly and indirectly. The direct effects are confined to the removal of sediment from the beach, often depositing the material on sand dunes. The indirect effects are through the creation of waves and also the setting-up of the local sea level (increased storm surge). Local coastal currents can also be created by winds which may be important in moving sediment (King, 1972 in Bernabeu *et al.*, 2003). Variations in wind direction would alter the nearshore current circulation, and such alterations might eventually become apparent in shoreline changes (Carter, 1975).

Fitting together all these variables and increasing their intensity, the morphological changes are often larger than long intervening periods of fair weather conditions, with storms being among the most important driving forces causing rapid and dramatic changes in beach morphology (Forbes et al., 2004; Balsillie, 1986, Morton, et al., 1995 and Morton, 2002). As stated by Balsillie (1986), storm effects depend on local wave refraction-diffraction patterns, sediment supply to the coast, beach morphological behaviour, dune development, human alterations and uses of the shoreline. In general, storms act on the sub-aerial beach and deposit the eroded material offshore, usually in the form of sandbars. Conversely, it is expected that during fair weather conditions bars slowly move back onshore (Niedoroda *et al.*, 1985; Backstrom *et al.*, 2009a).

Many studies have investigated the consequences of extreme single-storm events. However, beach vulnerability to storm action is also partly dependent on the difference between storm frequency and beach recovery period, whereby beach erosion is accentuated when storm frequency exceeds the beach recovery period for individual storms (Morton et al., 1995). In this case, a storm group exists and is defined as a series of successive storms without beach recovery in between. The definition of a storm group

depends, therefore, on the ability of a particular coastal area to recover from storm events (Ferreira, 2006). Interest in the consequences of storm group incidence on coastal evolution and morphology is relatively recent. Even if successive storms are common in some coastal regions, their cumulative impacts are still poorly understood (Birkemeier et al., 1999, Morton, 2002 and Ferreira, 2006). It has been recognised, however, that successive storms can cause significant erosion and important morphological changes (Lee et al., 1998 and Birkemeier et al., 1999). Furthermore, it has been observed that in some cases the combined erosion of successive storms is greater than the sum of the average erosion of the individual storm (Morton et al., 1995 and Lee et al., 1998). Ferreira (2005) concluded that the erosion caused by a group of storms with short return periods can easily exceed the single-event erosion associated with a longer return period storm.

Despite the importance on beach morphology actuation, observations of storm response on high energy beaches are still rare in comparison to accounts of storm impacts on low energy coasts. Cooper et al. (2004) believe that this could have been due to the infrequency of morphologically significant events on high-energy coasts, where larger storms might be required to produce morphological impacts. Short & Trembanis (2004) also pointed to the fact that coastal monitoring at higher temporal and spatial resolution carries many challenges including high costs with beach survey and also intense labour work because they typically require several years of data before meaningful trends emerge.

Closely linked to the beach morphological behaviour numerously cited above, and defended by many researchers, such as Dean (1991), is the control exercised by sediment texture and grain size. Beach slope, which is related to the grain size of the sediment (Carter, 1988 in Storms et al., 2002), determines the morphodynamic beach behaviour, where dissipative and reflective beaches mark the two extremes of this morphodynamic continuum, with a series of intermediate types in between (Wright & Short, 1984) Reflective beaches, argued by many to be caused by sediment deficit (Storms et al., 2002), are characterised by a narrow and steeply sloping surface with slope angles ranging from 6° to 10°. Beach sediment is usually characterised by medium to coarse gravel on the upper and lower beach face. These beaches typically comprise a step feature at the base of the swash zone, and beach cusps may be present on the upper beach, occasionally

fronted by a shallow sub-tidal terrace. In contrast, dissipative beaches are known to be almost entirely dominated by a flat, wide, featureless intertidal zone. Beach slopes are very gentle (0.5–1°) and composed of homogeneous fine to medium sands. This beach state is also known to have multiple breaker lines that dissipate the majority of their wave energy in the very wide surf zone (Harris et al. 2011 and Scott et al., 2011). Intermediate types may exhibit a combination of both types of the above mentioned. They are usually defined by the presence or absence, nature and form of sand bars and rip currents in the surf (Harris et al., 2011 and Short, 2006). As such, it could be expected a relationship by which dissipative beaches suffer lesser effects from storm's action, due to the presence of bars that provide efficient obstacles against energetic waves, than intermediate or reflective beaches (Carter & Balsillie, 1983). Likewise, reflective or intermediate beaches reduce their ability to dissipate energetic waves and as a result, they would be more sensitive to storm action (Benavente et al. 2000).

Despite this expected link between reflective / dissipative beaches and their behaviour when affected by extreme events, it is easy to check through some investigation results that morphologic changes can be diverse, proving that there is no simple relationship between high energy forcing and beach morphodynamic state. i.e., there are reports of different beach responses to storms incidence, such as the case where important damage was produced by means of overwashing (Benavente et al. 2002), and other cases where no significant damage was produced whether before or after these rigorous conditions, exhibiting a state of dynamic equilibrium. For example, Aagaard et al. (2005) observed beach profiles without significant changes arguing that the beach was already in equilibrium with energy conditions. Newe et al. (1999 in Aagaard *et al.*, 2005) obtained similar observations but concluded that morphological changes of beaches are related to the initial beach profile, where gentle slopes tend to have small changes. Wright (1980) also suggested that dissipative beach erosion is mainly limited to dune/backshore zone without any significant change of beach surface. In the same way, a study led by Benavente et al. (2002) indicates that beach predisposition to erosion depends mainly on the ability of beaches to change their morphodynamic state. In other words, seasonal beaches are more resistant to storms than uniform unchanging beaches. They justified their idea by saying that the drifting from one morphodynamic state to another one is

directly related to the beaches ability to adapt its profile to new energetic conditions. This autodefensive behaviour depends mainly on the amount of sand available for the change. They also verified that in places where there was not enough sand for the beach to acquire a complete dissipative state, the beach was severely eroded. The same authors concluded that the location of river mouths and other contouring conditions, favours a greater availability of sand in some beaches which, from a morphodynamic point of view, become more mobile and self-protected against storms. More recently, Almeida et al. (2011) investigated variations in beach morphology at the Praia de Faro (Portugal) and their relationship to wave conditions. They verified that morphological changes in this intermediate to reflective beach profile were greatest at the beach face/berm and sub-tidal terrace.

It becomes clear that the physical reasons why beaches sometimes erode, sometimes accrete, and sometimes are in a state of dynamic equilibrium over the time scale of one or more storm events or tidal cycles have not yet been determined (Aagaard et al., 2005). Even with this lack of knowledge, it is widely accepted that the morphology of a beach is mainly controlled by temporal variability of wave climate, tide and sediment characteristics (King, 1972 in Bernabeu *et al.*, 2003).

Since the beach and its behaviour are complex, and due to the lack and difficulty in collecting daily beach morphological and hydrodynamic data, several numerical models have been developed. Despite this wide range of numerical models, several authors have stated which fundamental parameters and steps a model should include: i) offshore wave height and wave period; ii) water level, including wave set-up; iii) representative grain size or fall velocity for the profile; iv) representative initial shape of the profile, including the dune; v) onshore boundary conditions for dune erosion; vi) calculation procedure for the cross-shore sediment transport rate or, alternatively, direct calculation of the morphologic change of the profile based on a given idealised form; vii) calculation procedure for computing dune erosion, containing a temporal dependence; viii) verification with field data over the range of conditions for which the model will be applied; iv) and storm surge duration (Balsillie, 1986; Kriebel & Dean, 1993; Van de Graff, 1994 and Schoones & Theron, 1995).

After a detailed analyses of different models and their application, it was concluded by Ferreira & Dias (2000) that it was virtually impossible to define conclusively which model(s) was superior to the others. However, the XBeach tool, developed to model the nearshore response to hurricane impacts, which includes wave breaking, surf and swash zone processes, dune erosion, overwashing and breaching, has been applied successfully along more complex situations. In the latter case, the coast has significant alongshore variability, and included the effect of sediment sorting, on including onshore processes (e.g. skewness, asymmetry), on modelling hurricane impacts over larger 2D areas, on predicting infragravity motions on coral reefs, on modelling short-wave motions and on modelling gravel beaches. The potential of the model strategy has been positively shown in a number of analytical, lab and field cases and is being used by a rapidly increasing user group worldwide.

Apart from these numerical models, a variety of indicators can also be used in to understand beach evolution. An example of data that can be used as an indicator of coastal state is the beach volume, defined both across the intertidal portion of the beach and across the full nearshore zone (Southgate, 2008). Many other indicators can be applied to comprise beach dynamics such as the identification of erosion and accretion phases on the beach, quantification of long-term recession and/or accretion trends, the degree of erosion and rate of recovery due to storm events, the beach response to engineering work, seasonal changes and interannual variability (Masselink & Pattiaratchi, 2001; Kroon et al., 2008 and Harley et al., 2011).

To select indicators from the above expressed variety, the knowledge of the coastal monitoring resolution and extension, performed at each study, is required. According to van Rijn et al., (2003), long-term trends are relevant for the evaluation of final beach width or the rate of erosion. Medium-term responses, with seasonal winter–summer profile oscillations, provide information about the cross-shore dimension of the berm. Finally, short-term changes (i.e., following an extreme storm) may determine the maximum retreat of the shoreline.

2.2 GIS TOOL FOR COASTAL DYNAMICS ANALYSIS

GIS provides spatial analysis and data integration techniques for accurate mapping and analysis of beach dynamic, dunes, wetlands, coastal bays and estuaries, and many other coastal features (Allen et al., 2012). It also allows to improve the knowledge on factors that control coastal behaviour, to evaluate the impact of forcing factors on littoral environments and manage them properly (Li et al., 2000). Furthermore, GIS provides simple access of data, ease edit and update, and fast visualization of coastal hazards (Bossak et al., 2005).

Since GIS was one of the tools recommended in the World Coast Conference in 1993 (Vellinga & Klein, 1993), a number of different projects using GIS applications for coastal zones, that allow coastal researchers to visualize coastal features in a much more intuitive way, have been developed (Andrews et al., 2002). An example is the Dune Hazard Assessment Tool developed by NOAA Coastal Services Center, (2003), a tool that helps coastal managers to identify the relative risk to properties from coastal erosion which use remotely sensed elevation data and traditional ground survey data.[1]

Numerous studies have explored GIS' potentialities in a variety of scenarios. To assist in the calculation of coastal change rates. For example, Duffy & Dickson (1995) produced an ArcInfo Macro Language program, SHOREGRID, that calculates shoreline evolution rates from digitized 2-D shorelines for two time intervals. SHOREGRID can also be used to predict future shorelines based on a linear projection of the calculated erosion rates. SHOREGRID has been successfully implemented to investigate sea cliff retreat (Moore & Griggs, 2002).

Similar to the SHOREGRID program, the Digital Shoreline Analysis System (DSAS) utilizes digitized shorelines in a GIS environment to quantify shoreline change. This tool uses regression techniques to calculate the linear change rates at specified locations between multiple digitized shorelines by casting perpendicular transects from the original shoreline (Harris et al., 2005; Himmelstoss et al.. 2006 and Pendleton et al., 2004).

[1] http://www.csc.noaa.gov/magazine/2002/01/news.html

Although not focused on erosion, Bossak et al. (2005) developed a GIS tool, the Coastal Impact Assessment Tool (CIAT), to predict the effect of coastal storms on beaches and dunes using beach slope, wave height, wave period, and tide/storm surge values. Additionally, the tool utilizes 3-D visualization features in GIS for scenario evaluation. The tool calculates estimated water run-ups during storms, which provides useful information for an assessment of likely coastal damage during storm events (Olsen, Young, & Ashford, 2012). It also incorporates a capability to access multiple data layers rapidly, including DEMs, Digital Raster Graphics (DRG), and aerial photography (Bossak et al., 2005).

The GEOSTORM Tool was developed by Almeida et al. (2011) to model beach erosion due to storms. This tool consists of a Graphical User Interface (GUI) that was written in Visual Basic for Applications (VBA) code, embedded in ArcMap (version 9.3). The tool comprises two modules: The first module enables the achievement of beach transect information; and the second module estimates profile erosion, at each transect, through the application of the Kriebel & Dean (1993) storm erosion convolution model (Almeida et al., 2011).

Applying 3-D analysis, the TopCAT tool provides a user-friendly interface for automated volumetric change analysis of large topographical datasets along with several tools to enhance DEM and Light Detection And Ranging (LIDAR) data processing. Results from TopCAT reveal erosional hot spots and alongshore coastal change trends for a region. As this GIS extension incorporates the use of a 3-D environment, working with TopCAT and 3-D data provides several advantages compared to 2-D data. First, TopCAT is not limited to transects, but instead works with the entire data grid thereby accounting for the data between transects. Next, a vectorized approach requires the user to select a consistent location for comparative analysis. Finally, TopCAT allows for continuous volumetric analysis which provides valuable information for sediment budget analysis (Olsen et al., 2012).

Frias et al., (2013) developed a Web GIS tool (WebInletAnalyst) that allows both researchers and managers to autonomous extract the evolution of key tidal inlet parameters such as minimum cross-section area, inlet width, maximum depth and migration distance, from a set of bathymetric charts and raw data surveys. The tool is

built on a web interface written and compiled using MatLab (The MathworksTM). Ultimately, the tool will be made available on Python code, allowing future further improvements and adaptations by the scientific community.

The GIS toolbox MAPBeach – GIS tools for Morphological Analysis at Pocket Beaches – was developed to simplify the morphological analysis of pocket beaches after morphological monitoring performed trough topographical surveys. The developed GIS toolbox enabled a quick and efficient evaluation of the morphological changes occurred at the selected beaches, associated to different forcing conditions, through the determination and further analysis of a set of pre-defined morphological parameters, including beach profiles, beach slope, elevation, volumes, beach curvature, beach rotation, among others. MAPBeach includes two sections: The single beach tool, which allows a simple characterization of the beach face along the entire area and determines the dominant beach directions and the radius of curvature in an easy way; and the Multi beach, that presents a greater complexity in implementation. The great advantage of this tool is to enable direct analysis and visualization of spatial and volumetric changes through altimetry comparison (Horta et al., 2013).

Despite the wide range of tools capable of examining beach morphologies, there are still some improvements to be considered, particularly in the case of lower spatial resolution data. On this basis, the GIS tool presented in this Dissertation has been created. This tool, created using the module Arcpy from Environmental Systems Research Institute (ESRI) ArcGIS®, takes in DEMs as input within an undefined number of *shapefiles* (data obtained from DGPS). Subsequently, it obtains beach profiles and volumes along defined lines that indicate the precise location of the profile to be extracted. In other words, this tool has very similar characteristics to the Graph Profile - 3D Analyst tool from ESRI ArcGIS®, adding the possibility of introducing numerous *shapefiles*' points (which depend exclusively on the computer processing power that will be used), and consequently obtaining areas and volumes from that portion of the beach. With this tool it is also possible to smooth the distribution of points obtained with DGPS along the beach and their associated inaccuracies as well as the continuous volumetric analysis, not just limiting the study to transect. This method is also described in detail ahead at chapter 4.

CHAPTER 3

3 STUDY AREA

3.1 GEOMORPHOLOGY

Five Finger Strand, a bedrock-framed beach, is located on the north coast of the Inishowen Peninsula, North of Donegal in the Republic of Ireland (Figure 3.1). This beach extends for approximately 1.7 km north-south between Five Finger rock and the mouth of Trawbreaga Bay (O' Connor et al., 2009).

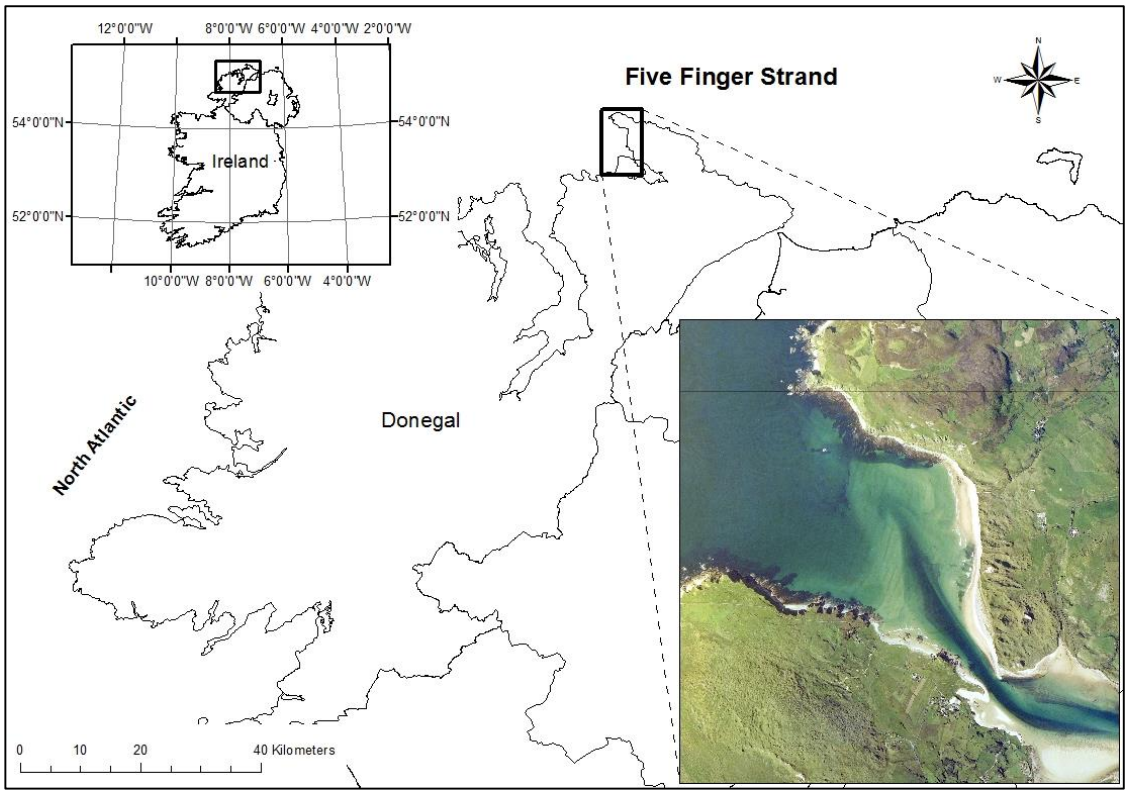

Figure 3.1: Study Area location. Font: Ana Luísa Martins.

Affected by successive glaciations, the Midlandian glaciation and ice limits during deglaciation are the main constraints on contemporary coastal geomorphology. Sediment supply occurs predominantly from reworking of shelf sands, and locally from erosion of bluffs of glacial sediments(Cooper et al., 2004). Coastal sediment supply is thus strongly related to patterns of ice movement, stabilisation and decay during the last glacial cycle (Jackson et al., 2005). Consequently, this embayment comprises a finite sediment volume with minimal longshore sediment exchange with other beaches and low contemporary sediment supply from other sources like rivers and primary productivity (Jackson & Cooper, 2010).

The beach is composed of a 2 m veneer of mainly fine sand (mean grain size 0.22 mm) with some medium sized sand along the dune line in the northern beach section and a subsurface pebble/gravel layer. It is geologically constrained between two rock headlands and fronts an extensive mature vegetated dune system. This dune system precludes barrier overwash during storms and constrains coastal morphological response to storms to cross-shore or alongshore transport of sediment under wave action and aeolian deflation and transport (Cooper et al., 2004).At the southern end of the beach a tidal inlet dominates the system and is associated with an ebb tidal delta and a tidal channel(Cooper et al., 2007). Within this estuary system modern fluvial sediment contribution is negligible and the main sediment exchanges take place between tidal inlet, tidal deltas, beach and dune (Jackson et al., 2005).

The northern beach is ≈ 350 m wide and dissipative at low tide and narrows to ≈ 90m at the southern end with a steeper slope. The dominant element at the southern beach area is the Trawbreaga Bay tidal inlet. The inlet throat is 100 m wide and is fixed in position, except seaward of the throat, in which the inlet position varies from a southerly position to northwesterly (Cooper et al., 2007). The ebb tidal delta position is also variable with relict shoals evident after the inlet position changes (O' Connor et al., 2009). The switch from one 'attractor' to another may occur over a relatively short time period. Previous studies have suggested numerous factors which may contribute to this change in tidal inlet behaviour, among these are Walton and Adams (1976) in O'Connor *et al.,* (2011) which proposed that the inlet had one stable position from which it was perturbed by fluctuations in external energy conditions reflected in average storminess rather than individual

storms. The system then returned towards its stable condition by internal sediment redistribution and onshore bar migration.

These findings contrast with those of Cooper et al., (2007), who suggested that the inlet was not stable and that the system continuously switched between the northwesterly to southerly position in a system of self-organization independent of external forcing. It was also stated that wave action causes increased sediment elevations at the seaward crest of the ebb delta reducing the efficiency of ebb currents, causing a deflection of ebb channel flow around the terminal lobe of the delta. The channel takes a new position and the former ebb delta is abandoned, and this sediment is reworked onto the adjacent beach. The relatively closed nature of the system with minimal sediment input means that once the ebb channel switches position to the south the sediment in the abandoned ebb delta is reworked onshore. Lack of modern sediment input coupled with the loss of some sediment into the flood delta results in progressive erosion, so the system cannot fully recover to its pre-erosional state. Cooper et al., (2007) also indicate that long-term, large-scale coastal behaviour can occur through normal day-to-day processes, i.e., it is not necessary to invoke sediment influxes, climate change, sea-level change, or extreme events as drivers of change. In short, when the inlet is in the northerly position sediment is removed from the beach and stored in the ebb tidal delta. This results in dune scarping, beach lowering and gravel exposure. In contrast, when the inlet position lies in the south the sediment is reworked and migrates onshore in the form of bars. This then results in beach accretion and dune progradation (Cooper et al., 2007 and O'Connor et al., 2010). It was also verified that previous phases of erosion and accretion of inlet position can lead to a shoreline position variation of ≈ 120 m.

Historical evidence from maps and air photographs records the occurrence of several erosion-accretion phases linked to the position of the ebb channel with fluctuations between these two states of approximately 25–50 years intervals. Superimposed on this cyclicity appears to be a gradual historical retreat of the shoreline as accretion following each successive erosional period does not regain the position of earlier shorelines (Cooper et al., 2007).

More recently, O'Connor et al. (2011) proposed that the channel relocation is the consequence of increase in average storminess conditions. They affirmed this based on

the peaks in North Atlantic Oscillation (NAO) values during 1900 to the mid-1920s, late 1940s to early 1950s, and the mid-1990s which suggested increases in wind speeds and wave heights, corresponding well to changes in channel positions. Thus, there appears to be a potential link between channel relocation and periods of high average storminess reflected in instrumental records and/ or NAO Index values.

3.2 HYDRODYNAMICS

High energy wave climate is predominant at Five Finger Strand. Records obtained by two offshore buoys (M4 Buoy (54840V N, 09804V W) was used to define Irish Sea wave conditions as the M2 Buoy (53838V N, 5825V W) described Atlantic wave conditions). Annual averages of wave height and period from the M2 and M4 buoys points to dominant swell waves with a modal significant offshore wave height of ≈2.2 m and a period of 9 s (Jackson et al., 2005), quite similar to those obtained using the data ERA-Interim (Figure 3.2). Equally, the dominant swell approach is from the W and SW quadrants (Figure 3.2), as also indicated by Cooper et al. (2007). The same authors moreover confirmed that waves are fully refracted upon reaching the beach. The swell refraction over the irregular sea floor and around the indented shoreline has produced a beach equilibrium plan form that typically shows little net morphological change on an annual basis and is also stable in the medium term (Cooper et al., 2004).

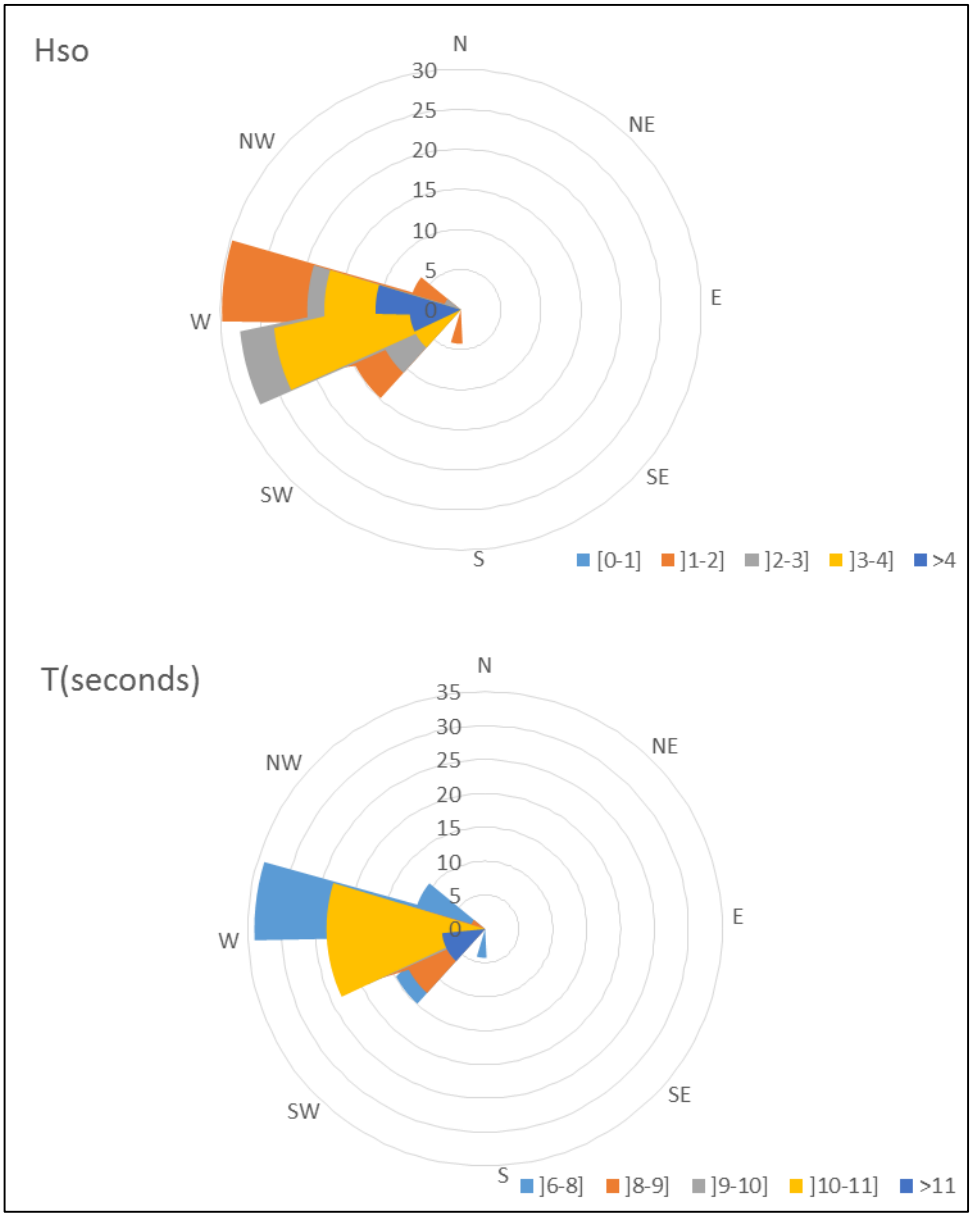

Figure 3.2: Wave climate during the study period. Font: ERA-Interim data (see subchapter 4.4).

The existing planform configuration can be easily modified by the actuation of storms. Due to the intersection of the main conduit of North Atlantic cyclones, Ireland experiences the maximum impact of Atlantic swell waves and storm activity (Jackson & Cooper, 2010). With dominant winds from the SW quadrant, winter storms generate deep-water waves whose heights can reach 15–20 m (Carter & Balsillie, 1983 and Jackson & Cooper, 2010), and are refracted significantly southwards as they encounter the northwest coast of Ireland (Backstrom et al. 2009).

Similarly to this refraction effect, distinct factors also limit the morphological impact of storms and the identification of their impacts in the study area. First, because the coastline is exposed to modally high energy swell that arrives fully refracted at the shoreline, an increase in swell size may not necessarily create a change in wave energy dispersal patterns. Instead, analysis of the impact of increased swell size using wave modelling suggests that much of the excess energy is accommodated by development of a wide surf zone with much wave energy dissipation offshore. In contrast, short period waves associated with locally strong winds, dissipate their energy further shoreward, where they are not fully refracted and may thus be more effective in generating gradients of wave energy that lead to alongshore or offshore sediment dispersal (Cooper et al., 2004). Second, since the sandy beaches are in the dissipative morphodynamic domain, much long-wave- length wave energy is dissipated across the shoreface during increased swell regimes and is unlikely to generate an excess of energy in the nearshore (Cooper et al., 2004).Third, because the tidal range is mesotidal, with spring tide of ≈ 3.5 m and neap tide ≈ 1.6 m (Cooper et al., 2004; Jackson et al., 2005 and Backstrom et al., 2009), there is a long tidal interval during which short-lived storms will not coincide with such levels, causing a reduced occurrence of elevated water levels that exceed normal tidal high water levels (Cooper et al., 2004).The duration of a storm will thus enhance its likelihood of spanning a high tide level. Fourth, offshore sediment losses during storms are likely to be replaced by fair-weather swell conditions. Thus, long-term impacts of storms are likely to be difficult to detect in the historical record of morphological change except at the vegetation line (Cooper et al., 2004).

The study carried by Cooper et al., (2004) revealed a strong spatial variability in potential shoreline response to storms. For these authors, for a storm of high enough magnitude to cause morphological change, factors such as wind direction, coastal orientation, interaction of wind and swell waves, produce potentially important differences in coastal response patterns.

Cooper et al., 2004 also revealed that relatively few storms have produced coastal morphological impacts over a 40–50-year period. They linked this few storms actuation with the wind, once it can optimize the transfer of energy to waves, which in turn undergo refraction, reflection and dissipation as they approach the shore (Cooper et al., 2004).

Sea-level change can also operate as a direct forcing factor generating morphological change on an open-coast beach (Storms et al., 2002). Carter (1982) speculated that a slightly falling relative sea level might explain the dune progradation observed at Five Finger Strand in the late 1970s and early 1980s. The sea-level record since then is, however, considerably more complex and includes fluctuations that do not show a clear link to the observed morphological changes (Jackson et al., 2005).

3.3 COASTAL MANAGEMENT PRACTICE

The 'problem' of erosion at Five Finger Strand began in the mid-1990s with shoreline erosion, dune scarping, beach lowering and gravel exposure (Cooper et al., 2007). Concern for the beach by the general public and local councillors was countered by the construction of a small seawall (approximately 10 m wide) in the mid-1990s authorised by the local authority engineer at the time, to protect the car park (O'Coonor et al., 2010). However, no maintenance was carried out on the seawall and it subsequently failed due to continued beach lowering and dune scarping (Cooper & Mckenna, 2008).

The undeveloped nature of the Five Finger Strand hinterland meant that pressure to halt the erosion at the site was mainly the result of a desire to maintain present conditions and preserve its recreation-friendly state. The initial construction of the seawall demonstrated that hard sea defences would not provide the answer to the erosion issue (Cooper & Mckenna, 2008).Hence, general public and local councillors determined that the introduction of hard artificial engineering structures in response to public demands at the site would have resulted in wave reflection and consequent beach lowering, gravel exposure and ultimately the loss of sand from the beach. Fixing the position of the dunes would also have accelerated erosion elsewhere, particularly at the edges of the armoured sections. Cutting off the dunes from the sediment exchange system would have halted the natural working of the system once dunes provide the sand storage buffer which is part of the "defence mechanism" of beaches in response to storms. Without this supply of sediment the beach seaward of the defences would lose its natural protection, resulting in erosion and sediment starvation. The placement of artificial structures would also have destroyed the visual quality of the site (Cooper & Mckenna, 2008).

Since coastal erosion continued to be a problem, with increased intensity at the beginning of this century, possibly due to a number of high magnitude storms, it was accepted that hard engineering was not a sustainable option but a system of soft intervention could be adopted. As a pilot scheme straw bales were used as a form of coastal protection (Figure 3.3) (O'Connor *et al.*, 2010).

Figure 3.3: Straw bales used as a form of coastal protection. Font: O'Connor *et al.*, 2010.

In order for any soft engineering methods to work, the method chosen must be appropriate for the individual site. It was accepted by the engineer and coastal scientists that placement of straw bales at Five Finger Strand would not halt the erosion, but it was seen as a low-cost, temporary response to ease public pressure at the time. The bales were emplaced in November 2005 and one section was replaced in 2006. As a form of dune protection the bales did not stop the retreat of the scarp, but they stayed in place for over a year without affecting the ability of the coast to operate naturally (O'Connor etal. 2010).

The perceived slowing of the erosion rate, coupled with the management action taken, quelled the pressure for artificial hard defences. Since 2004 the onshore movement of sediment from the ebb delta has increased beach levels and resulted in mainly sandy conditions, which are more acceptable for recreation purposes (O'Connor et al., 2010). This lead to the recognition that the erosion at this site is part of a longer erosion/accretion cycle. The system, since then, has continued to work naturally (O' Connor et al., 2009).

CHAPTER 4

4 METHODOLOGY

4.1 FIELD SURVEY

Morphological surveys were performed on Five Finger Strand beach, Northern Ireland, over an eight year period, between February 2004 and January 2012. Surveys were undertaken regularly, at intervals of approximately two months or after a storm, always performed at low tide and preferentially during spring tides, totalling 75 beach surveys. Eight shore-perpendicular profiles spacing each other approximately 200 m (Figure 4.1) were monitored using a DGPS. The base station was set up over a known temporary benchmark while the rover was attached to a quad (Figure 4.2). The DGPS was then used to stake out all profiles by inserting 2 poles on the line of each profile. These poles were then lined up at low water and the quad driven inland along the profile to the base dune collecting X, Y and Z data every 1 m. The DGPS provides an accuracy of ±3 cm in the vertical and horizontal dimensions, giving a high level of accuracy for monitoring beach profiles.

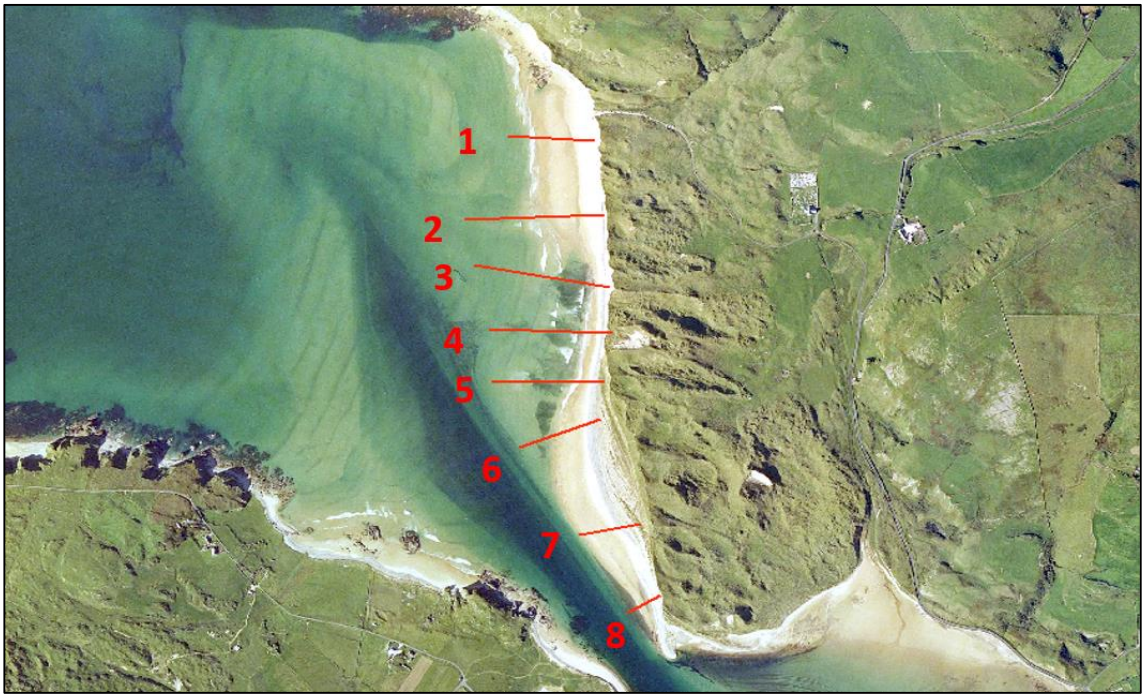

Figure 4.1: Shore-perpendicular profiles used as DGPS survey' guide.

Figure 4.2: Field survey with DGPS' rover attached to a quad.

The coverage of beach elevation points varied slightly due to different conditions of sea waves and tides, having reached approximately1000 elevation points for each survey; a total area of 182752 m^2, a minimum value of altitude of -2 m and maximum of 4 m, relatively to the mean sea level.

4.2 DATA PRE-PROCESSING

Despite requiring a short amount of time at the site, field measurement of elevation along transect lines only measures one- and two-dimensional changes (change in elevation along X or Y). It does not effectively represent the spatial variability of beach topography in the system statistically or cartographically because of the horizontal distance between transects. As a result interpolation is used to predict these values for which there is no recorded observation within the area covered (Algarni & El hassan, 2001). The development of a digital gridded continuous surface, or DEM, suitable for landform analysis and modelling, can be done using readily available basic mapping software. However, the selection of interpolation method is more complex, requiring both visual and statistical exploration (Andrews et al., 2002), since there is no explicit rule indicating which method is adequate for a particular surface (Erdogan, 2009). The choice of the interpolation method and its parameters depends on the type and characteristics of the surface to be generated, the type of surface to be modelled along with the purpose of the modelling, and also on the accuracy, density and distribution of the source data (Gong et al., 2000 and Yılmaz, 2007).

Due to its extensive use, DEM quality are particularly important, and must be an important input when using and comparing methods for particular applications (Smith et al. 2003). The accuracy of interpolation methods can be evaluated by different methods. One of them is the split-sample method. In this method some raw data are omitted, interpolation is performed, and the difference between the predicted and measured values of the omitted values is calculated. This difference is used as a measure of the stability of the interpolation algorithm (Smith et al., 2005).

In order to enable such a validation method, within the *ESRI ArcGIS*® software the function “Subset Features” from the “GeostatisticalAnalyst” was used. This extension allows a random division of the data into two parts: the "training" for DEM creation and the "test" for its validation. Thus, the data were divided in two parts: 95%for the "training" which were tested with different interpolation methods, and the remaining 5% for the "test" which enabled an assessment of the methods by comparing the interpolated values with the values obtained from the field survey.

A total of 13 interpolation methods were tested using for each one the options that best fit the field data. The differences between the interpolated and observed elevation values at each "test" point were analysed using standard descriptive statistics for DEM accuracy assessment(Fischer & Tate, 2006). The most common statistical descriptor is the Root Mean Square Error (RMSE) (Li, 1988 and Fischer & Tate, 2006):

$$\boldsymbol{RMSE} = \sqrt{\frac{\sum(\boldsymbol{Z_{DEM}} - \boldsymbol{Z_{OBS}})^2}{\boldsymbol{n}}}$$

Where Z_{DEM} represents the interpolated elevation from the DEM, Z_{OBS} the observed elevation and *n* the number of sample points.

Two other descriptors, the Mean Error (ME) and the Error Standard Deviation (S), are used frequently for a more complete statistical description of DEM interpolation error (Desmet, 1997 and Fischer & Tate, 2006):

$$\boldsymbol{ME} = \frac{\sum(\boldsymbol{Z_{DEM}} - \boldsymbol{Z_{OBS}})}{\boldsymbol{n}}$$

$$\boldsymbol{S} = \sqrt{\frac{\sum[(\boldsymbol{Z_{DEM}} - \boldsymbol{Z_{OBS}}) - \boldsymbol{ME}]^2}{\boldsymbol{n-1}}}$$

The two extreme values for the difference between the interpolated and observed elevation (positive maximum and negative maximum) were also retained, indicating the general location of all other values (Li, 1988). Visual representation of models was also taken into account on the definition of the best method since it is also important to consider how the method represents reality in visual terms. Thus, to choose the best method it was also visually verified the capability of the methods to represent the morphology when compared to field observations (visual reliability).

The results for the descriptive statistics, presented in Table 1, indicate that despite the sparse data distribution, some methods have good statistical results. The best method chosen to represent the data/ beach over the years was the Radial Basis Function (RBF),

Multiquadratic. This method consists on a series of exact interpolation algorithms in which the surface passes through each measured sample location. It is conceptually similar to fitting a rubber membrane through the measured sample values while minimizing the total curvature of the surface. According to Yang et al. (2004), Multiquadratic function is considered by many to be the best interpolation method.

Table 1: Statistical results for Interpolation Methods.

	Interpolation Method	Model	Visual Reliability	ME	RMSE	S	Positive	Negative
	Triangular Irregular Network (TIN)		*	0.5384	1.1090	1.0013	3.4890	0.0085
	Natural Neighborhood Interpolation (NNI)		*	0.5572	1.1141	0.9964	3.4890	0.0088
	Inverse Distance Weighting (IDW)		*	0.2837	0.4424	0.3506	1.3466	0.0003
	Local Polinomial Interpolation (LPI)		*	0.3511	0.5624	0.4537	1.9417	0.0368
Radial Basis Functions	Completely Regularized Spline (CRS)			0.1749	0.2919	0.2413	0.8434	0.0014
	Spline with Thension (ST)			0.1591	0.2677	0.2224	0.7728	0.0007
	Multiquadratic (M)		*	0.1042	0.1873	0.1607	0.5885	0.0025
	Inverse multiquadratic (IM)			0.2341	0.3651	0.2894	0.9877	0.0075
	Thin Plate Sline (TPS)			0.0805	0.1581	0.1406	0.5050	0.0011
Kriging	Exponential	Ordinary (KEO)	*	0.1148	0.2002	0.1695	0.6074	0.0012
		Simple (KES)		0.2456	0.3615	0.2739	0.8918	0.0031
		Universal (KEU)	*	0.1147	0.1997	0.1688	0.6096	0.0022
	Gaussian	Ordinary (KGO)	*	0.1708	0.2976	0.2517	0.9710	0.0037
		Simple (KGS)		0.1344	0.2060	0.1612	0.6123	0.0025
		Universal (KGU)	*	0.1642	0.2796	0.2337	0.9074	0.0031
	Circular	Ordinary (KCO)	*	0.1068	0.1894	0.1615	0.5839	0.0025
		Simple (KCS)		0.1750	0.2606	0.1994	0.6638	0.0163
		Universal (KCU)	*	0.1072	0.1860	0.1569	0.5733	0.0027
	Spherical	Ordinary (KSO)		0.1081	0.1895	0.1608	0.5861	0.0029
		Simple (KSS)	*	0.1871	0.2819	0.2178	0.7113	0.0013
		Universal (KSU)	*	0.1082	0.1890	0.1601	0.5827	0.0027

As important as the choice of interpolation method, the optimum cell size must be also evaluated. The optimal dimension of DEM grid size, or resolution, is a function of the morphologic feature under investigation and computing capacity (Hengl, 2006). For example, if the mapped feature is relatively homogeneous, a small grid cell size may introduce artifacts that are not there. Grid cell size can also be too large not representing correctly the details of the morphology. The enlargement of grid resolution leads to aggregation or up scaling and decrease of grid resolution leads to disaggregation or downscaling. As grid becomes coarser, the overall information content in the map will progressively decrease and vice versa (McBratney, 1998; Kuo et al., 1999 and Stein et al.,2001). So grid resolution should also be dependent on the purpose of the analysis (Andrews et al., 2002).

Although much has been published on the effect of grid resolution and the accuracy of spatial modelling, choice of grid resolution is seldom based on the inherent spatial variability of the input data (Bishop et al., 2001 and Vieux & Needham, 1993). In fact, in most GIS projects, grid resolution is selected without any scientific justification. In the ESRI ArcGIS® package, for example, the default output cell size is suggested by the system using some trivial rule: in the case where the point data is being interpolated in Spatial Analyst, the system will take the shortest side of the study area and divide it by 250 to estimate the cell size ([ESRI], 2002).

Therefore, to test the cell size that best fits the existing data three different methods were used. The first one was adapted from the cartographic rule which says that there should be at least one (ideally four) observation per 1 cm^2 of the map. This Scale Number (SN) method, known as "Inspection Density" (Hengl, 2006), can be expressed mathematically as:

$$SN = \sqrt{\frac{A}{N}} \times 10^2$$

Where A is the surface of the study area in m^2 and N is the total number of observations.

The second method is also mentioned by (Hengl, 2006) and connects the problem of the grid resolution with the Nyquist–Shannon sampling theorem. This theorem indicates that a suitable grid resolution can be derived for given sample elevations (e.g. contours) and

based on the complexity of terrain. Hence, the grid (pixel) size (ρ) should be at least half the average spacing between the inflection points:

$$\boldsymbol{\rho \leq \frac{l}{2 \cdot n(\delta z)}}$$

Where l is the length of a transect and n (δz) is the number of inflection points observed.

Lastly, the "Point to Raster" tool in ESRI ArcGIS® was used by consulting the default cell size for the output raster dataset. The default cell size is the shortest of the width or height of the extent of the input point data, divided by 250.

The results obtained by the three methods showed an optimal resolution of 2 meters.

4.3 BeachProG – BEACH PROFILE GRAPH TOOL

Scripting in ESRI ArcGIS® environments is possible since the introduction of version 9. Realizing that many of their users do not want or need to be programmers, but would rather have some tools at their disposal to solve the problem at hand, ESRI has chosen to support a variety of scripting languages. One of the languages supported is Python (Butler, 2005). Python is a freeware programming language designed to be an easy-to-use, easy-to-learn dynamic scripting language. This means that there is no compiling, it is interactive and it allows users to learn its many layers of implementation at their own pace (Butler, 2005).

A script in Python language for ESRI ArcGIS® can be created in two ways. The first way is to export the existing model from ArcToolbox to the Python script. The export tool automatically imports module Arcpy (Dobesova, 2011).This module is a site package that builds on the successful ESRI ArcGIS® scripting module with the intention of creating the basis for a useful and productive way to perform geographic data analysis, data conversion, data management, and map automation with Python. With ArcPy it is possible to have access to geoprocessing tools as well as additional functions, classes, and modules that allow the creation of workflows quickly and easily. The second way is to directly create a script in an integrated development environment, in which basic program

structures such as cycles (for, while), and decision structure (if, else) can be utilized. It is also possible to add notification messages to result window for users about flow of the batch data processing. Moreover, some methods from Geoprocessor, like enumeration methods that return a Python list of all file names or raster data sets in a directory on hard disk, are only accessible by scripting (Dobesova, 2011).

The BeachProG tool has a range of functions that come with the package ESRI ArcGIS® and functions created for the specific purpose of this thesis, such as the beach profile volume calculation.

4.3.1 Tool Acquisition

The tool is in a zipped folder named BeachProG. This folder can be stored anywhere on the computer, however the path cannot contain spaces or underscores. The folder that contains the input data and the one created to receive outputs should also follow this requisite.

When extracting the files from the zipped folder the user will come across the folder structure in figure 4.3.

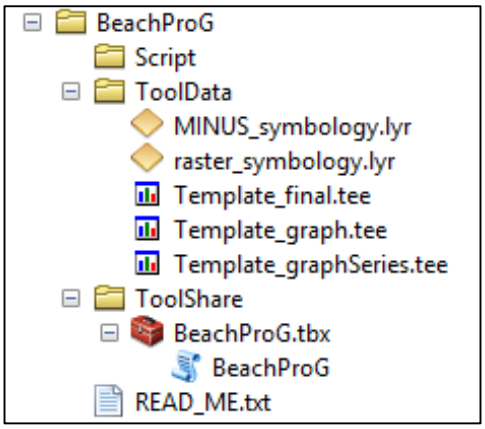

Figure 4.3: Folder structure of BeachPROG tool.

- The folder "Script" contains the script used to run the tool in ESRI ArcGIS®. The user must make sure that the path that the tool displays in ESRI ArcGIS® (through the properties of the tool in ArcCatalog) corresponds to the current path where the tool has been saved.

- The folder "ToolData" stores all the files needed to run the tool. In this case the layers are present with the definition of the colour palette to be used in DEM, and the templates used to create the beach profiles.
- The Toolbox containing the tool is in the "ToolShare". To use the tool in ESRI ArcGIS®, simply access this folder in ArcCatalog and double click "BeachProg". It will open the window of the input parameters. This window will be described in detail later.
- Also present in this folder is the file txt "READ_ME" containing the basic indications of tool's usage, the same information described in this subchapter.

As described above, the BeachProG tool executes the system tools from ESRI ArcGIS® in a sequence, feeding the output of one tool to the input of another. These tools are based on some extensions that depending on the type of user license of ESRI ArcGIS® can be present or not. There are three extensions in these conditions: "3D Analyst", "Geostatistical Analyst" and "Spatial Analyst". Users should therefore make sure that they have these three extensions.

In addition to the extensions, the version of ESRI ArcGIS® is also extremely important. This tool was developed using ArcInfo 10.1, so a version equal or superior to is extremely recommended.

4.3.2 Input Parameter Window

The interface between Python workflow and users is made through the Input Parameter Window (Figure 4.4).This parameter window allows the user to input data required to run the tool. Once the tool is executed, the parameter values are sent to the tool's source code. The tool reads these values and proceeds with its work.

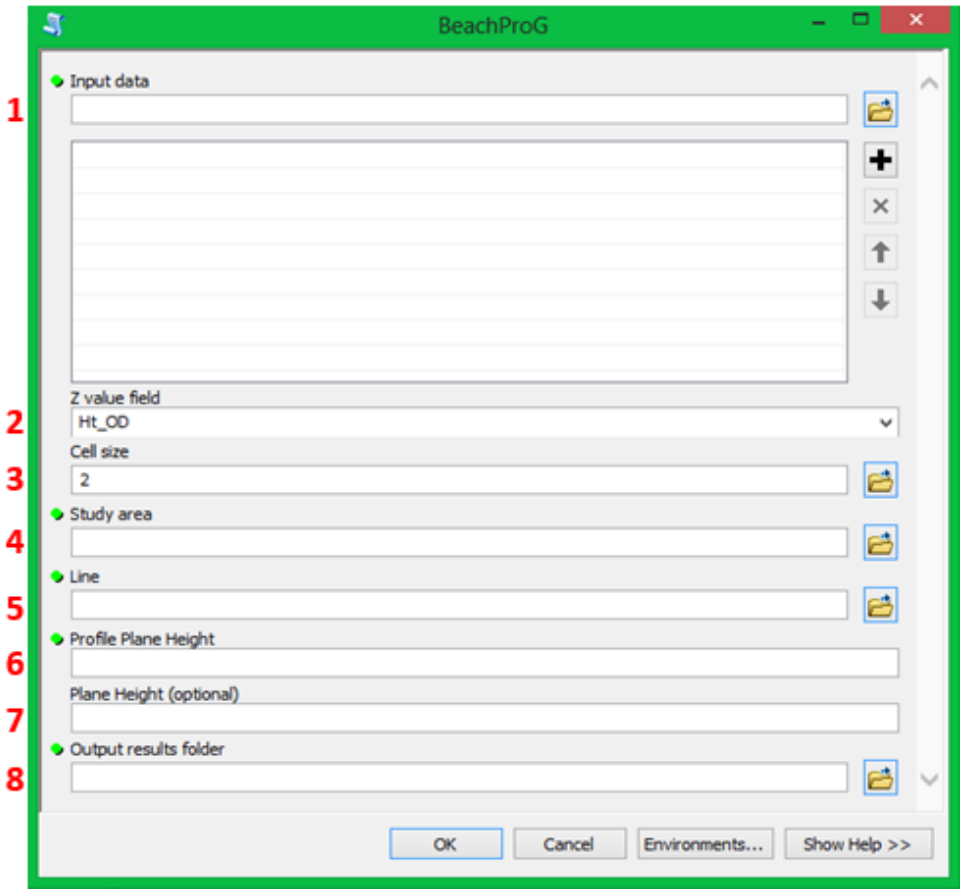

Figure 4.4: Input Parameter Window of BeachPROG tool.

For a proper use of the tool the user must follow the suggestions / conditions for completing the fields enumerated at Figure 4.4.

1. Input data - The input features containing the z-values to be interpolated. Only Feature Classes are allowed. This field allows the introduction of various features (Multivalue Parameter) at the same time, however the files must be entered in ascending / descending order, since some functions within the tool will be carried out taking into account this order. These data form the basis for the construction of DEM.
2. Z value field - Field that holds a height value for each point. This field name containing z-values must be entered by the user and the field's name must be equal for all *shapefile*s (introduced at step 1), otherwise the tool will result in an error.

3. Cell size - The cell size at which the output raster will be created. The default value is set to 2 (meters) based on studies that were conducted specifically for this work. However, it can easily be changed.
4. Study area - The feature used to clip the input features. This polygon sets the limits of the area to be compared with the other files (comparison over the years). This polygon will always be the same for all surveys.
5. Line - Input line mask defining the section to be extracted. This field refers to the line that will be used to extract the value of raster cells intersected by the line, for beach profile construction. The direction of this line will indicate the ascending or descending order of data plotted in profile graph.
6. Profile PlaneHeight - The elevation of the plane that will be used to calculate both area and volume from the beach profile graph. Volume and area will be calculated above the Profile Plane Height.
7. Plane Height - The elevation of the plane that will be used to calculate both area and volume from the raster. Volume and area will be calculated above the Plane Height. Heights are always the same for all surveys data.
8. Output results folder - The folder that will contain the results from Profile tool. The name should not contain spaces or underscores.

4.3.3 Structure of BeachProG

4.3.3.1 Data Pre-conditions

As this tool was created to specifically best fit the data obtained from the field work, it was necessary to understand the type of data in question and the steps necessary to achieve the objectives proposed for this tool.

Despite being collected with a DGPS system, the data obtained from the field work have spatial incoherence. As these data are the base for the beach profile extraction that will be compared along the years, the profiles must be always extracted at the same position. To circumvent this situation it was defined that the field data serve as the basis for DEM construction and afterwards the introduction of a line by the user will indicate the precise location for beach profile extraction ("Line" - Point 5 from Input Parameter Window). The example below (Figure 4.5) demonstrates this situation.

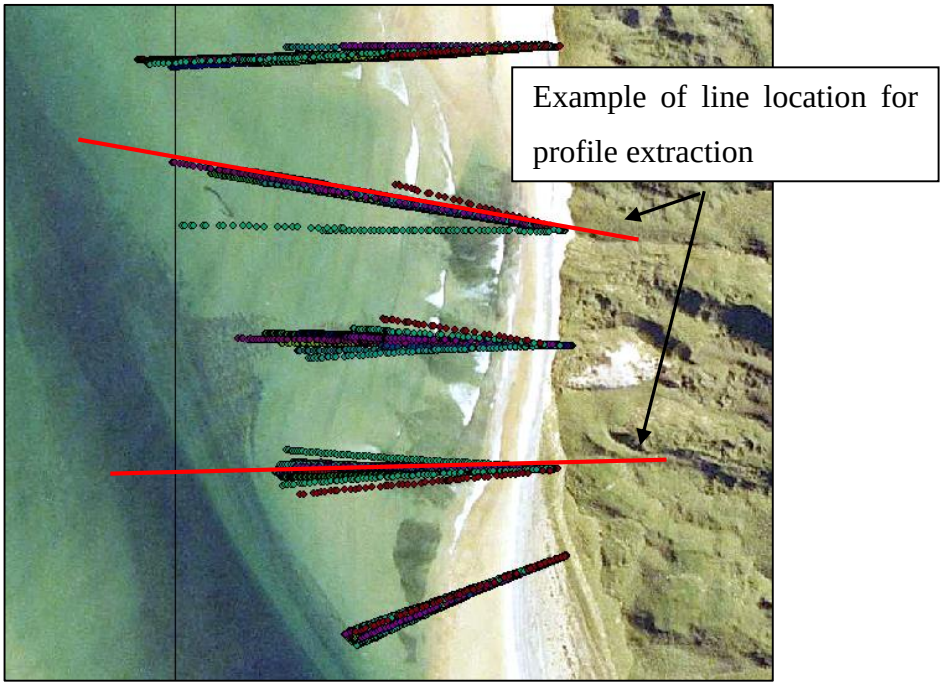

Figure 4.5: Spatial incoherence of DGPS surveys along time and example of a defined extraction line.

As the coverage of beach elevation points varied slightly due to different conditions of sea waves and tides and because it is necessary to always use the same area, for temporal comparison, a polygon was constructed ("Study Area" – Point 4 from Input Parameter Window). For this the following principles were considered: (i) For points to the East (next to the base of the dune), it was selected the farthest point from the base of the dune, for all common points between surveys (Figure 4.6); (ii) For the northern and southern limits of the polygon, the central points were chosen and were given a margin of approximately 1 meter to avoid null values when constructing DEMs (Figure 4.6); (iii) points to the West of the beach (seaward limit), the farthest points from the seaward limit were chosen, i.e., the points that were closer to the centre of the beach were chosen. Figure 4.6 illustrates the point selection to create the polygon (study area). Data length much greater or smaller than the remaining data were excluded from the study.

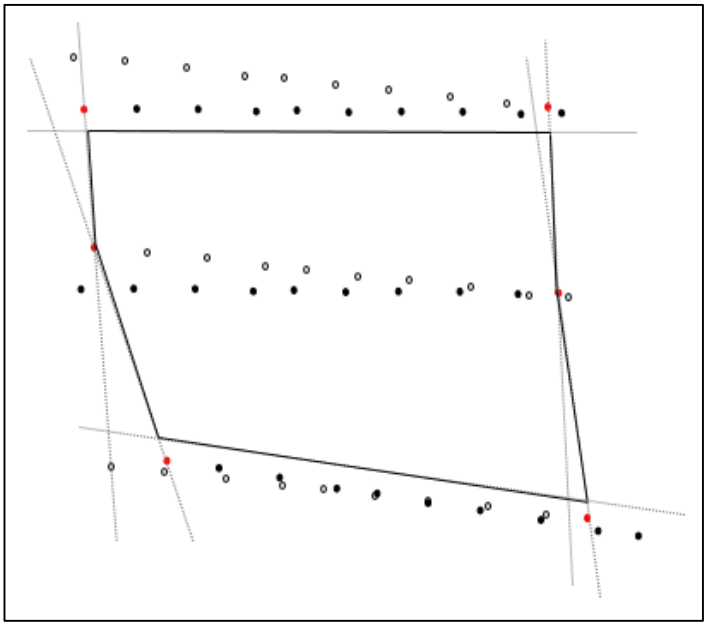

Figure 4.6: Illustration of point's selection to create the polygon for study area delimitation. The red dots indicate the points chosen for the creation of the polygon.

4.3.3.2 Script structure

The BeachPROG tool is a sequence of python functions. Once running this tool, the following tasks are performed:

1) Starting with the DEM construction, it is applied the best interpolation method for this beach surface representation, based on DGPS data (described in subchapter 4.2).
2) Sequentially, the polygon introduced in section 4 of the Input Parameter Window cuts the DEM obtained in step 1, defining the study area. In other words, the cells of the raster corresponding to the study area will be extracted. Informations outside the polygon are eliminated.
3) Through the line introduced in section 5 of the Input Parameter Window, it is extracted all raster cells that intersect the DEM from step 2).
4) For each cell of the raster from step 3, a middle point will be created in the output feature class and all raster cells information are attached to these points.
5) Determines the distances between points created in step 4. This distance is calculated from the nearest point of the basis dune to the remaining points.
6) Calculate area between consecutive points based on their distances and elevations.

In order to compare the results obtained over several years, the area (A) between subsequent pairs of profile points was calculated using:

$$\boldsymbol{A = \sum (\delta h_{LOW} \times d_{SUB}) + \left((0.5\ \delta h_{SUB}) \times d_{SUB}\right)}$$

Where:

δh_{LOW} = the difference in height between the lowest point on the profile and the lowest point of the subsequent pair that is being analysed;

d_{SUB} = the horizontal distance between the subsequent points being analysed;

δh_{SUB} = the difference in height between the subsequent points being analysed.

To simplify this calculation, the minimum height is always equal to zero. This is possible through the introduction of the "reference plane" that is given by the user, i.e., the minimum height from which the user wants to draw the profile. If the plan entered by the user is less than zero, the positive of this value is added to the others elevations, so that the minimum height is always zero (Table 3).

The total area is calculated through the sum of all values calculated in the previous step (Figure 4.7).

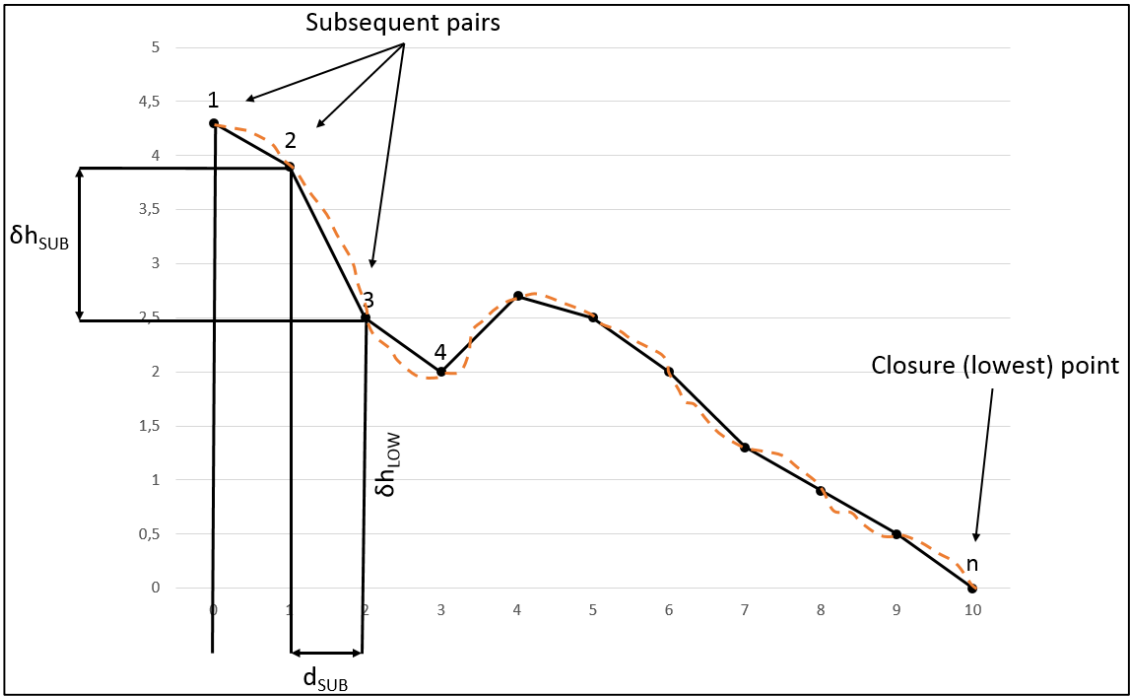

Figure 4.7: δh and dSUB calculation to determine the area (A) between successive points.

7) Creates a new raster based on subtraction of different surveys, such as 2012 minus. 2004 This step allows to identify changes that have occurred over this period, such as areas of erosion or accretion. So, it is subtracted the value of the second input raster from the value of the first input raster on a cell-by-cell basis.
8) Calculates the total area and volume of rasters from step 2 above the reference plane introduced in point 7 of the Input Parameter Window.
9) Creates a profile graph as a visual output using the graph template within the folder "BeachProG\ToolData".
10) Creates a profile series graph as a visual output using the graph template within the tool.
11) Converts a table with coordinates, area, total area and mean slope informations to a Microsoft Office Excel file. This can only be used with ESRI ArcGIS® 10.2

The figure 4.8 shows the sequence of functions used to obtain the BeachProG results.

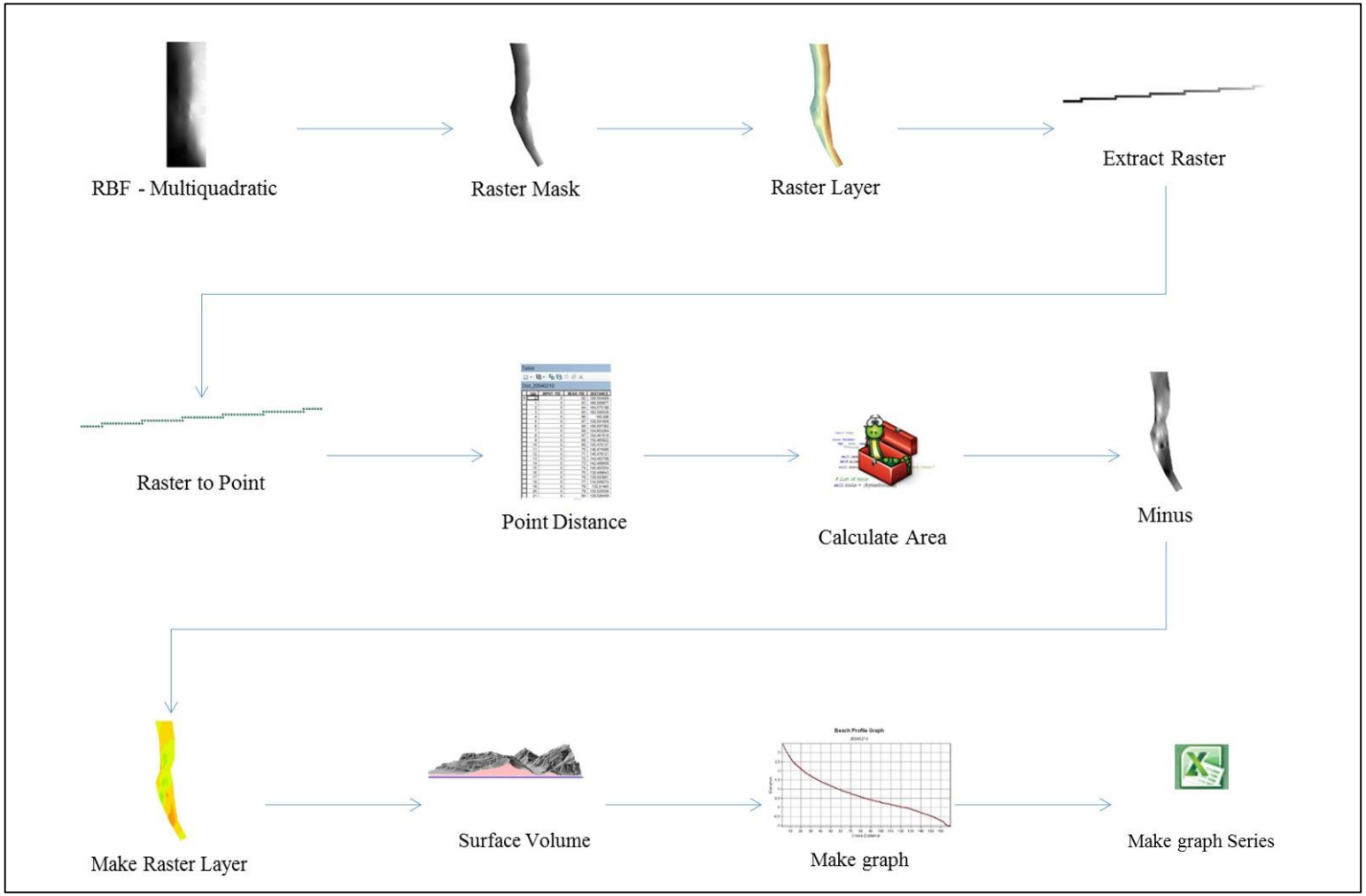

Figure 4.8: Sequence of functions used in BeachPROG tool

4.3.4 Tips for modification / customization

As this tool can be used with data from all coastal sites, and because this tool was created to fit the study area in question, it is necessary to pay attention to some situations:

- Because raster names cannot have more than 13 characters, the input data name (first field of Input Parameter window), must be modified. For this, all names should have the same structure, equal or similar to: "year" + "_" + "location". Then, a new name is created. The example bellow (Figure 4.9) shows the structure used for this work:

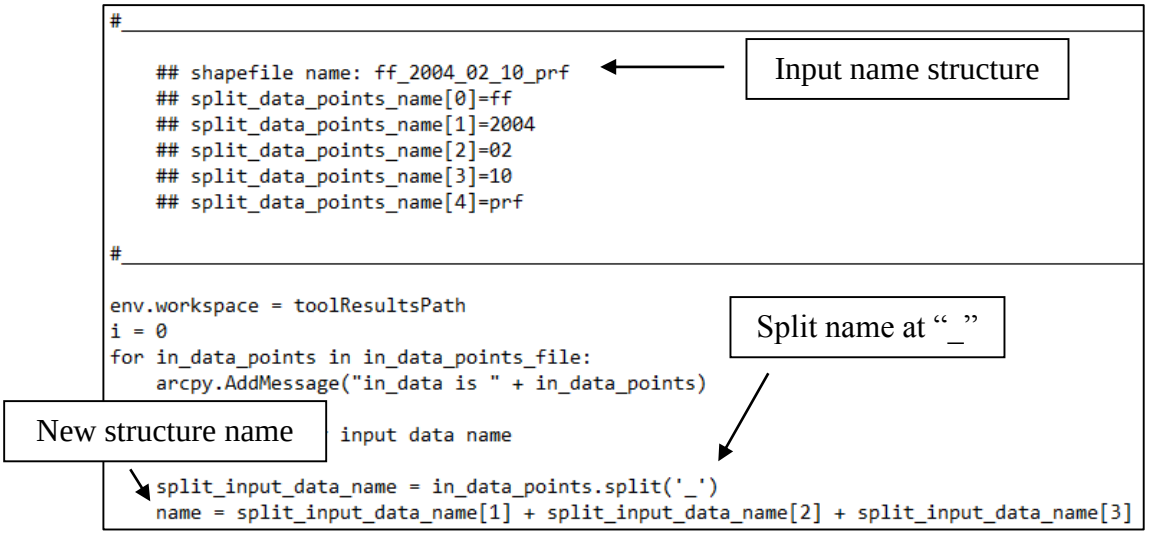

Figure 4.9: Code for modification of input data name.

- The type of model used to develop DEM should be modified if the user concludes that the Multiquadratic interpolation method does not efficiently represent the surface.
- The templates within the folder "ToolData" can be replaced. If so, the names should be the same in both script and folder (Figure 4.10).

```
#Get the path name to this script
scriptPath = sys.path[0]
#Get the pathname to the ToolShare folder
toolSharePath = os.path.dirname(scriptPath)
#Now construct pathname to the ToolData folder
toolDataPath = os.path.join(toolSharePath,"ToolData")
#Create the pathname to the graph template
templatePath = os.path.join(toolDataPath, "Template_graph.tee")
#Create the pathname to the graph series template
templategraphSeries = os.path.join(toolDataPath, "Template_graphSeries.tee")
arcpy.AddMessage("templatePath is " + templatePath)
#Now construct pathname to the RESULTS folder
toolResultsPath = os.path.join(toolSharePath,outputFolder)
arcpy.AddMessage("output folder " + toolResultsPath)
#Create the pathname to the raster symbology
RasterSymbologyPath = os.path.join(toolDataPath, "raster_symbology.lyr")
#Create the pathname to the minus raster symbology
MinusSymbologyPath = os.path.join(toolDataPath, "MINUS_symbology.lyr")
```

Figure 4.10: Code for templates and folders location.

- The last part of the script is the table conversion, with elevation, area and slope information, for Excel files. This is only available for version 10.2 of ArcGIS, so the user must delete or comment ("#") this part of the script if using older versions. Alternatively, this information can be accessed by opening the ".dbf" file of the *shapefile* in excel.

4.4 RELATIONSHIPS BETWEEN WAVE CONDITIONS AND BEACH VOLUME

Because of the difficulty in accessing wave data during the study period, results from a hindcast model were used. The enormous distance of M4 and K4 oceanographic buoys from Five Finger Strand beach and the discontinuity of their records favoured their exclusion. Hindcast is a way of testing a mathematical model against known values to reconstruct past conditions. This approach usually refers to a numerical model integration of a historical period where no observations have been assimilated. As observations of surface wave parameters such as the wave height (Hso) are relatively scarce, hindcasting is generally a successful alternative.[2]

[2] http://www.oceanweather.com/research/HindcastApproach.html

The hindcast data used here is based on stored data obtained from the weather observation, produced by the European Centre for Medium-Range Weather Forecasts (ECMWF). These data have become an important and widely utilized resource for the study of oceanic processes and predictability since they are produced using fixed, modern versions of the data assimilation systems developed for numerical weather prediction. Consequently, they are more suitable than operational analyses for use in studies of long-term variability.[3]

The data used here belong to ERA-Interim, which is the latest global atmospheric re-analysis produced by the ECMWF. It covers the period from 1 January 1989 onwards, and continues to be extended since March (2009) in near-real time to support climate monitoring (Dee et al., 2011).

The ECMWF forecasting system consists of several components: an atmospheric general circulation model, an ocean wave model, a land surface model, an ocean general circulation model and perturbation models for the data assimilation and forecast ensembles, producing forecasts from days to weeks and months ahead (Persson & Andersson, 2013).

The wave prediction system is based on the Wave modelling (WAM) approach (Komenet al., 1994) which concists in an optimal interpolation scheme to constrain predicted wave spectra using altimeter wave height observations (Dee et al., 2011). The sea state is described by the two-dimensional wave spectrum which gives the distribution of wave variance over different frequencies and propagation directions. Wave energy then follows from the product of water density, acceleration of gravity and wave variance.[4]

In a generic way, the methodology used to obtain oceanic data from ERA -Interim is:

- Obtain observations of relevant atmospheric parameters for meteorological models (atmospheric pressure, temperature, ice cover, among others);
- Introduce these atmospheric parameters in an atmospheric general circulation model which will use atmospheric pressure to simulate wind fields;
- The wind field is introduced in the ocean circulation model to generate waves;

[3] http://www.ecmwf.int/research/era/do/get/Re-analysis_ECMWF
[4] http://www.ecmwf.int/en/research/modelling-and-prediction/marine

- And finally, the sea surface wave is then integrated again in the atmospheric circulation model to simulate the roughness and friction of the ocean surface that will influence their own wind fields (called a two-way coupling of nested models).

This methodology runs successively each day and all the processes are restarted using the new atmospheric observations.

Since this is a model of global and oceanic range, wave climate conditions are always considered at deep water, i.e., the waves are always generated without considering energy dissipation by bottom friction and consequently increased wave height in shallow waters.

A more detailed information about the current status of ERA-Interim production, availability of data online, and near-real-time updates of various climate indicators derived from ERA-Interim data, can be found at ECMWF site.[5]

To have access to ERA-Interim data, a free download is available for a regular grid that covers the entire globe. For this specific case, information was extracted for the grid point closer to Five Finger Strand (Figure 4.11), at location of 55.5º and -7.5º. The point is about 20 km from the beach and has a water depth of approximately -58m.

The result is a table which contains records for all days and months related to the chosen period: 01-01-2004 to 31-12-2012 in this case. Each day presents four records with 6 hour intervals in between. Moreover, three types of data can be found, that are the swh - significant wave height (meters), mwp - mean wave period (seconds) and mwd- mean wave direction (º, starting at North).

The obtained wave data was compared against the volumetric values obtained for Five Finger Strand using the following methodology:

A. Interaction between wave action and beach volumetric behaviour. A qualitative analysis was performed based on graphical observation of the difference between beach volumetric results and maximum Hso over the years under study, allowing the observation of the behaviour / response of the beach in relation to wave action. For this, it were used the monthly average of Hso values, based on daily average,

[5] http://www.ecmwf.int/research/era

a month before the dates of volumetric surveys of the beach. This correlation helps to identify the environmental factors acting on the behaviour of the beach.

B. The effect of the channel - the channel can affect the volume of the beach significantly. To do this analysis, there were identified (with bibliographic resource), periods of significant variation of the channel to determine if they coincide with periods of increased volume variation of the beach.

C. The wave direction - the occurrence of sediment erosion / accumulation periods may be related to different wave direction. To relate this, the results obtained at point "A" were compared with the annual mean wave direction in order to try to get some behavioural patterns.

D. Occurrence of alongshore sediment transport. Part of the sediment can be transferred from one location to another alongshore resulting in a differentiation in response to wave propagation between profiles. That is, one profile can accumulate and the other one can suffer erosion, for similar offshore wave conditions, while the total variation of the beach may be zero. This indicates the occurrence of alongshore sediment transport. To verify this occurrence the data were divided into two groups according to the direction of wave propagation, which promote sediment transport in opposite directions.

E. Finally, the relationship between wave action and each beach profile volume was determined for the eight profiles through the use of linear regression, yielding a line of best fit and a significance level for the relationship. The calculated lines constrained the intercept through the origin assuming that there are no vertical variations when the Hso is zero. The resultant equations define the empirical relationships between offshore wave height and beach profile volume, which enabled a Hso threshold for important morphological changes to be calculated.

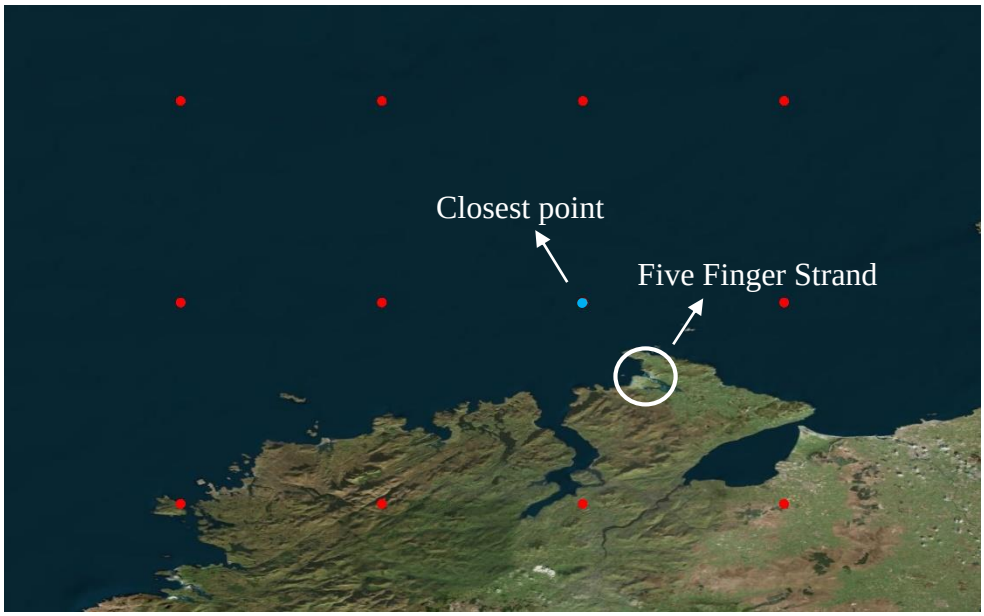

Figure 4.11: Grid data with the closest point (≈ 20 km) to Five Finger Strand. Font: ERA-Interim data image.

CHAPTER 5

5 RESULTS

5.1 BEACH VOLUMETRIC ANALYSIS

5.1.1 Total Volume

The results obtained with the tool enable an analysis of the beach evolution over the years under study. The first results obtained with this tool are the DEM. These DEM, although imprecise, due to the large spacing between existing profiles, allow a visual analysis of the beach behaviour. The temporal comparison allows a preview and general notion of erosion / accumulation locations and periods as well as the behaviour of the shoreline. Figure 5.1 allows a temporal visual analysis of results obtained in 2004, 2006, 2008 and 2012. It is possible to see an indentation of the shoreline in the northernmost part of the beach, while the southernmost part seems to move toward the sea. In the northernmost part of the beach, it is also possible to observe a decrease in intensity of the colour on the positive values indicating an altimetric variation, that is, the occurrence of beach erosion. Contrary, the southernmost part presents an accumulation tendency.

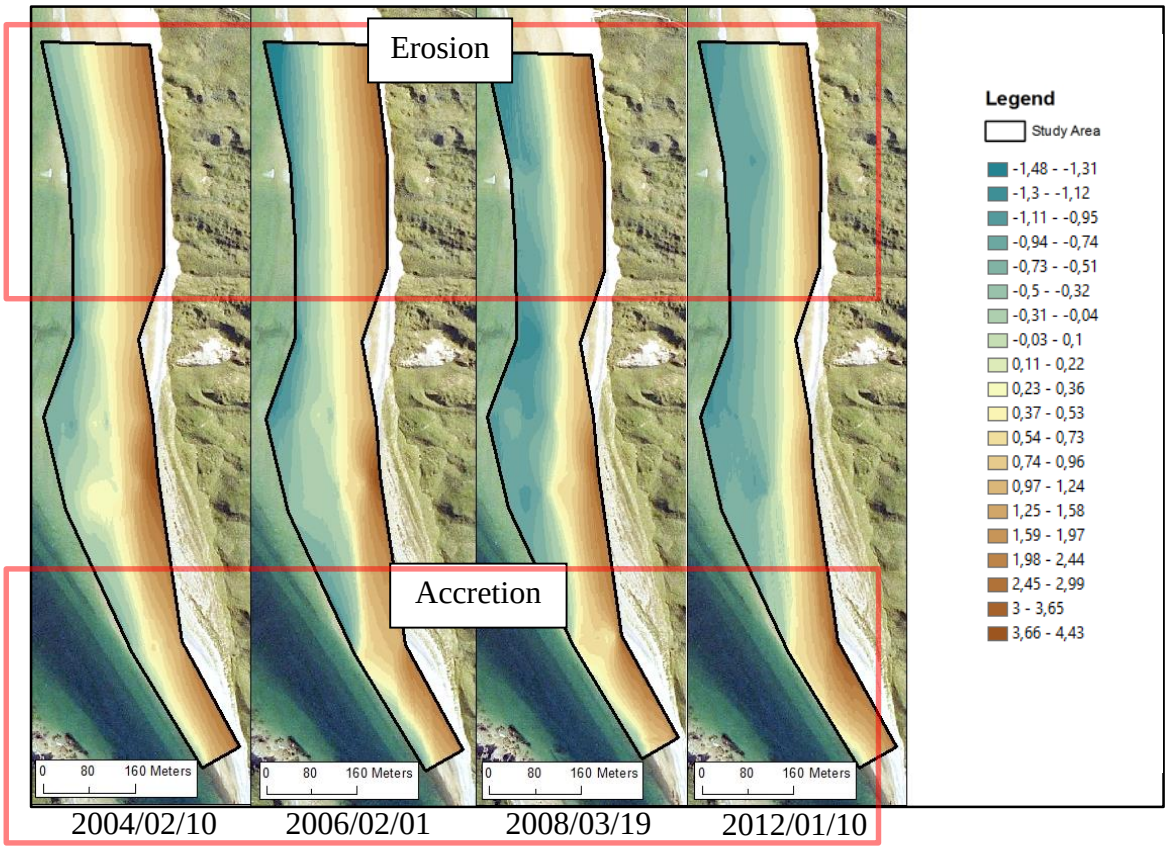

Figure 5.1: DEM changes along time for the study area.

To complement this visual analysis the tool produces an excel file with values of areas and volumes for all DEM produced. The transposition of these values to charts enables an easier volumetric analysis. The following chart shows the volumetric variation from 2004 to 2012 as well as the trend line of these values (Figure 5.2). The results indicate the occurrence of continuous coastal erosion with an average loss of ≈ -2000 m^3/year, despite the existence of some accretion periods, such as the volumetric accretion in 2007/11/09, while other are marked by erosion.

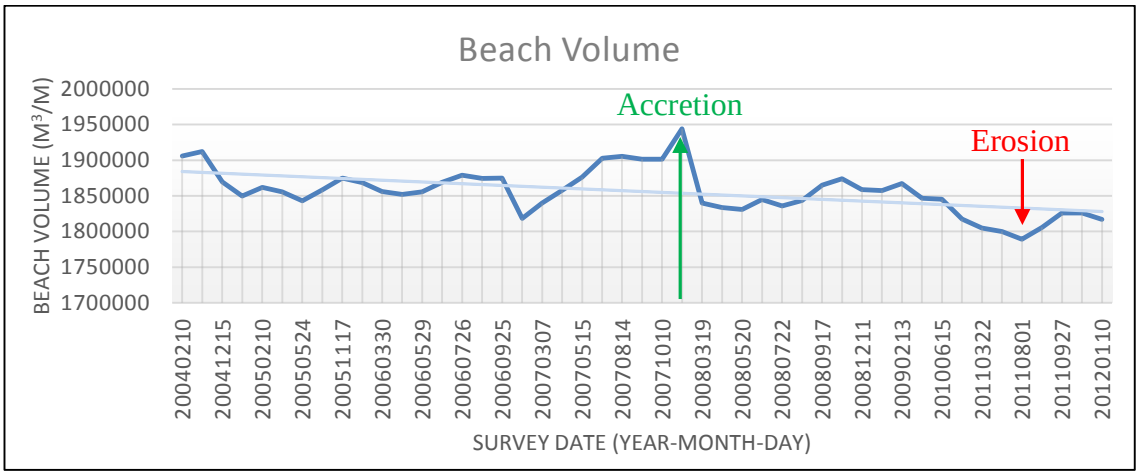

Figure 5.2: Beach volume changes from 2004 to 2012 and respective trend line.

By calculating the difference between the consecutive total volumes obtained in the same excel file, it is possible to identify periods of increased erosion / accumulation (Figure 5.3). Periods of increased erosion are related to 2004/04/07, 2006/09/25 and 2007/11/09, and the greatest accumulation occurred in 2007/10/10, with values of -42494 m^3; -56455 m^3; -104258 m^3 and 42779 m^3, respectively. The occurrence of a total erosion of circa 90000 m^3 was verified.

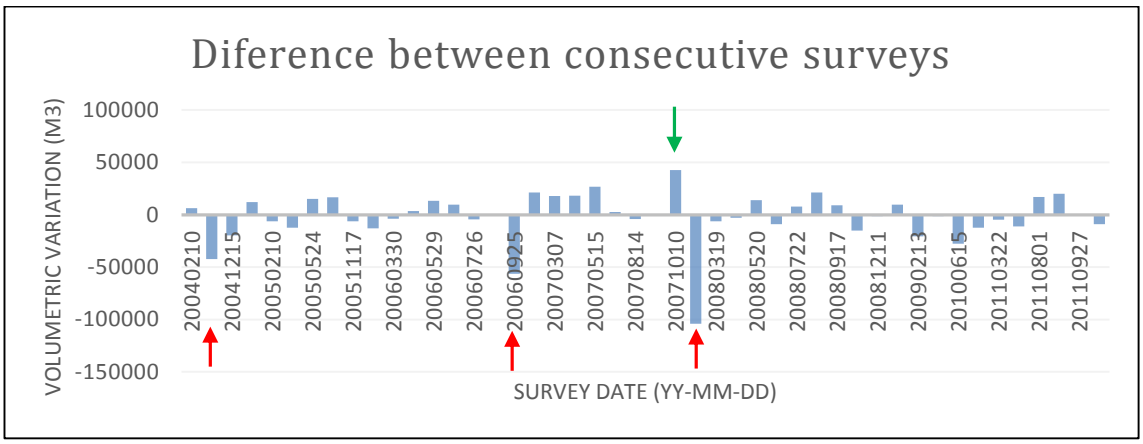

Figure 5.3: Volumetric difference between consecutive surveys.

Another approach taken by the tool is the DEM resulting from the comparison between consecutive surveys. This result allows the observation and easy identification of locations where sediment erosion / accumulation occurred. The DEM for the outcomes identified in the previous graph (periods of increased erosion and accumulation), are

present in Figure 5.4 below. The layer symbology was created so that the areas with higher erosion are shown in red, with a gradual change to green, where there are areas of sediment accumulation. The north and south parts of the beach suffer erosion.

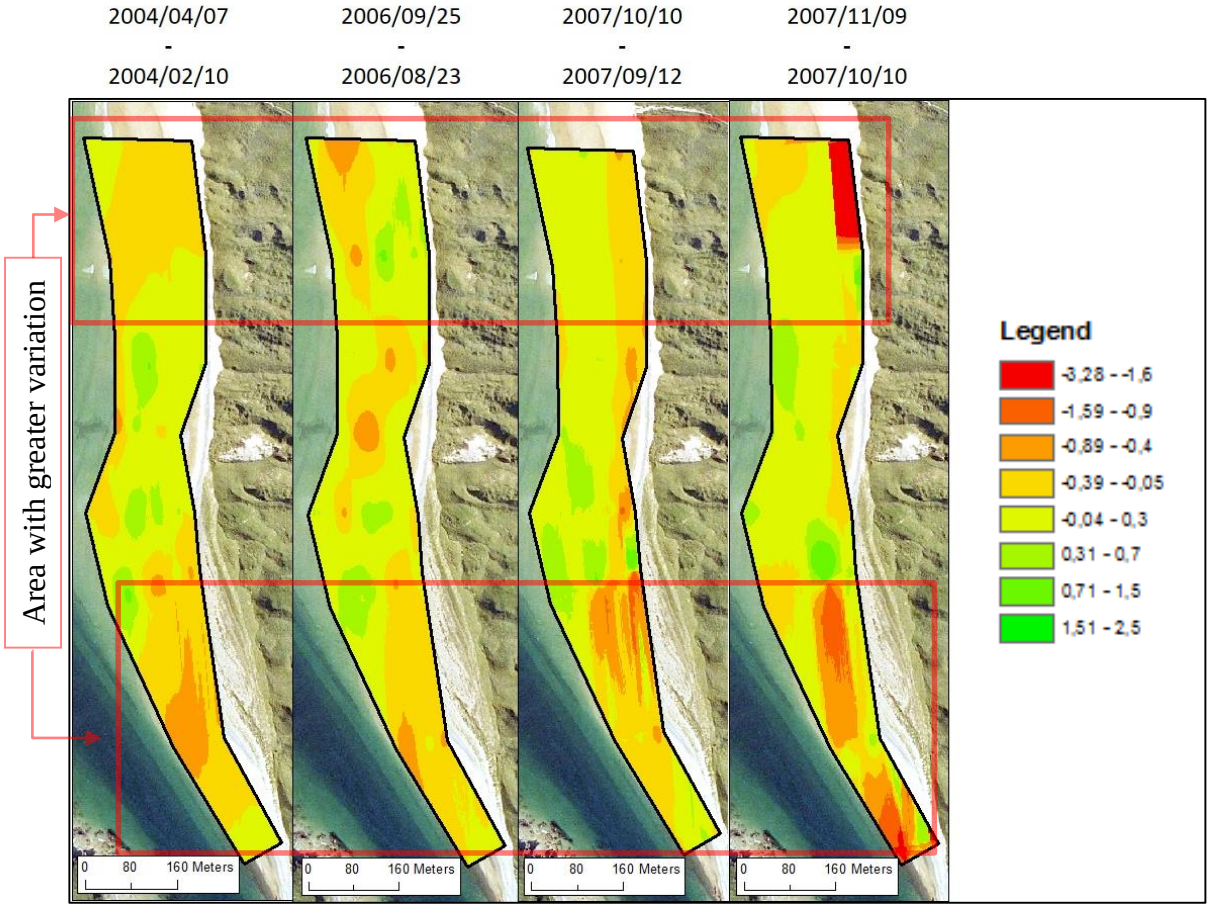

Figure 5.4: DEM resulting from the comparison between consecutive surveys and identification of locations where sediment erosion / accumulation occurred.

5.1.2 Beach Profiles Volume

For a more precise and detailed analysis of the beach volumetric variation, the beach profiles study revealed to be the best approach for this case study. Thus, the tool produces two results: excel table with the volume information for a quantitative analysis, and the profiles images for qualitative analysis. From the excel file it is possible to obtain the charts with volume variation of each profile (Figure 5.5, 5.6, 5.7 and 5.8). All profiles showed gradual erosion over the years, except for profile 7. Through the difference between consecutive volumetric variations it was possible to quantify the erosion and accumulation observed in profiles. The overall volumetric variation for the analysed

period was: erosion of 79,954 m^3 for profile 1; 65,538 m^3 for profile 2; 65,372 m^3 for profile 3; 31,910 m^3 for profile 4; 61,910 m^3 for profile 5; 100,471 m^3 for profile 6; 25,623 m^3 for profile 8, and an accretion of 58,288 m^3 for profile 7.

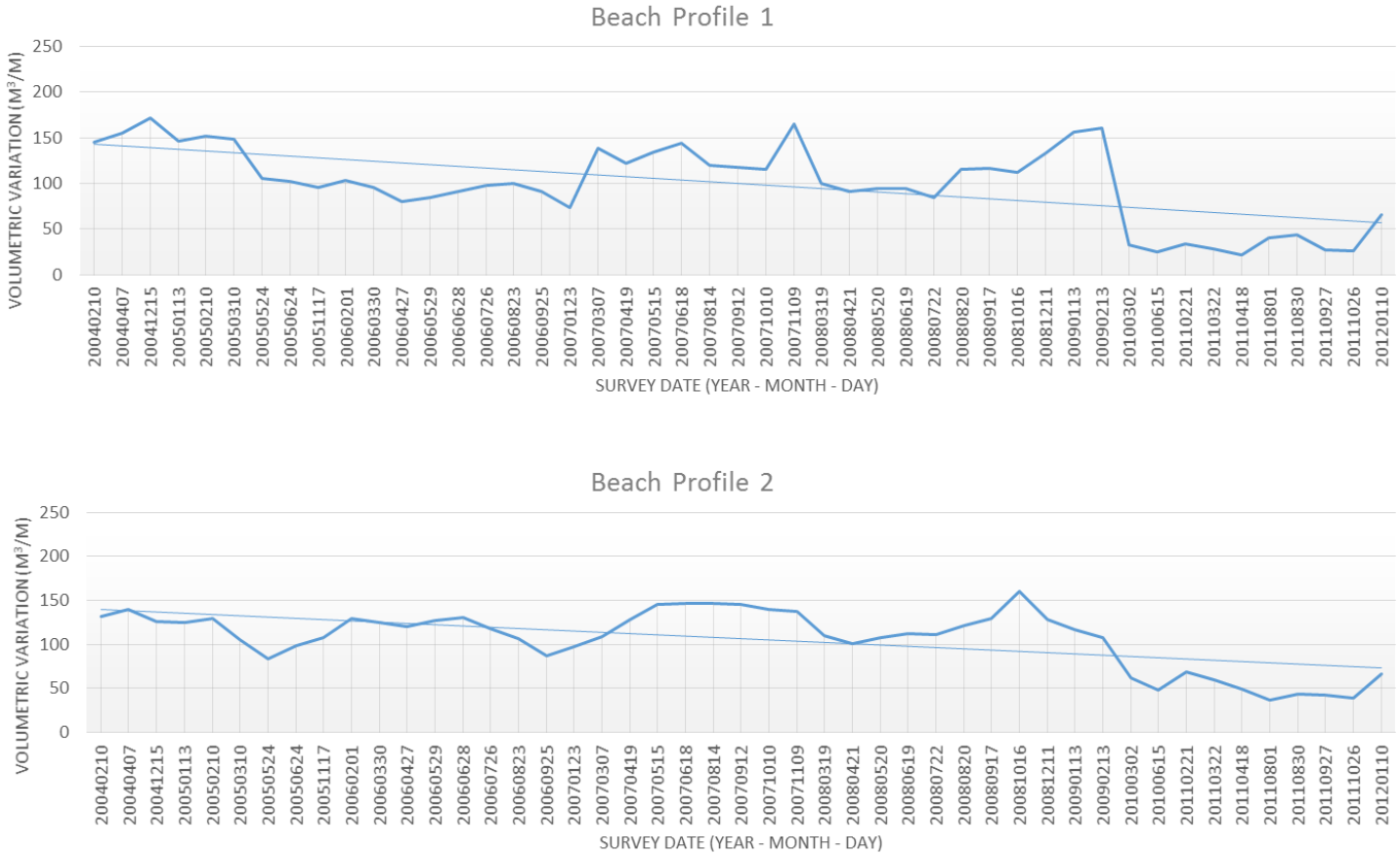

Figure 5.5: Beach Profiles volumetric variations during the study period.

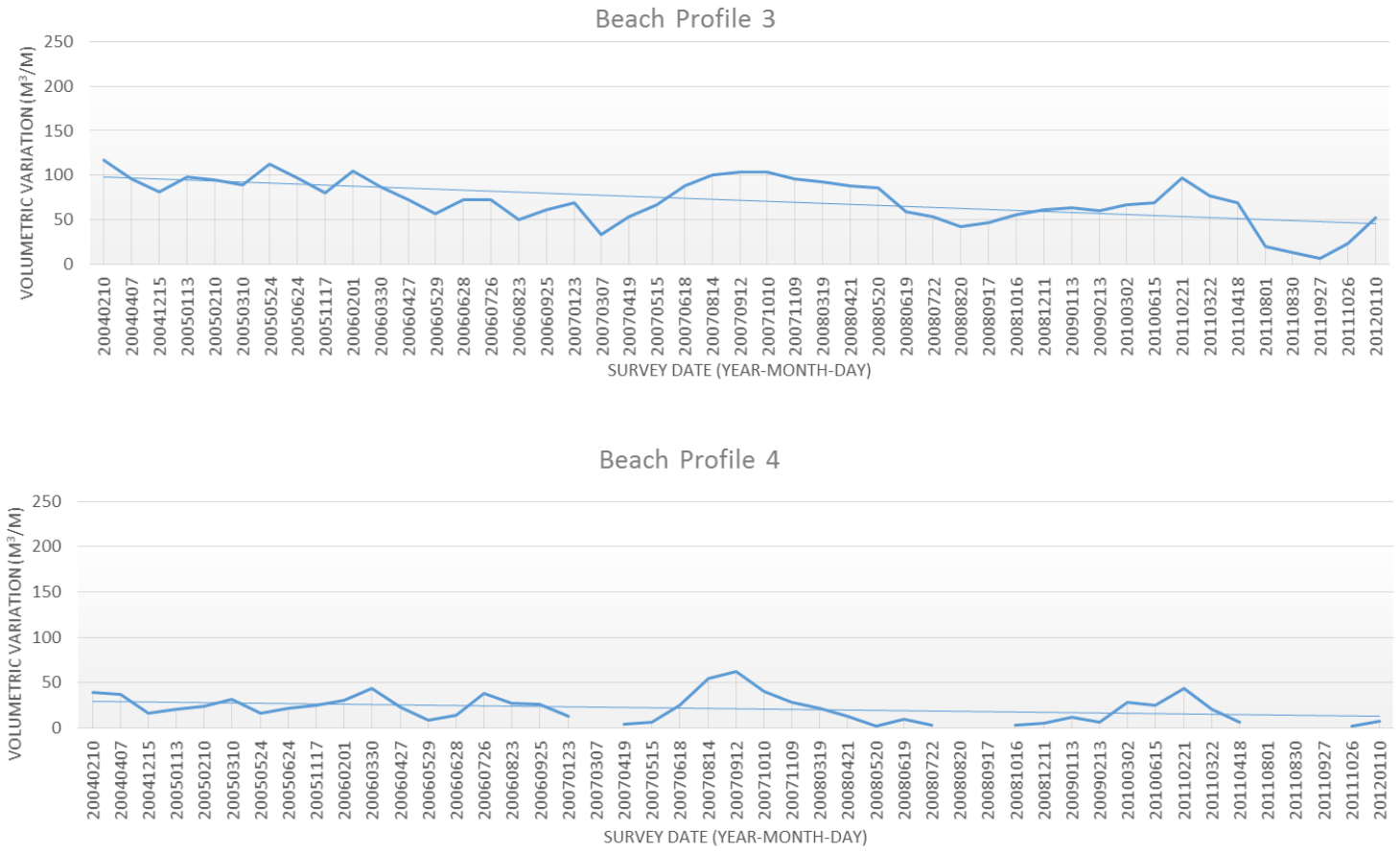

Figure 5.6 (Cont.): Beach Profiles volumetric variations during the study period.

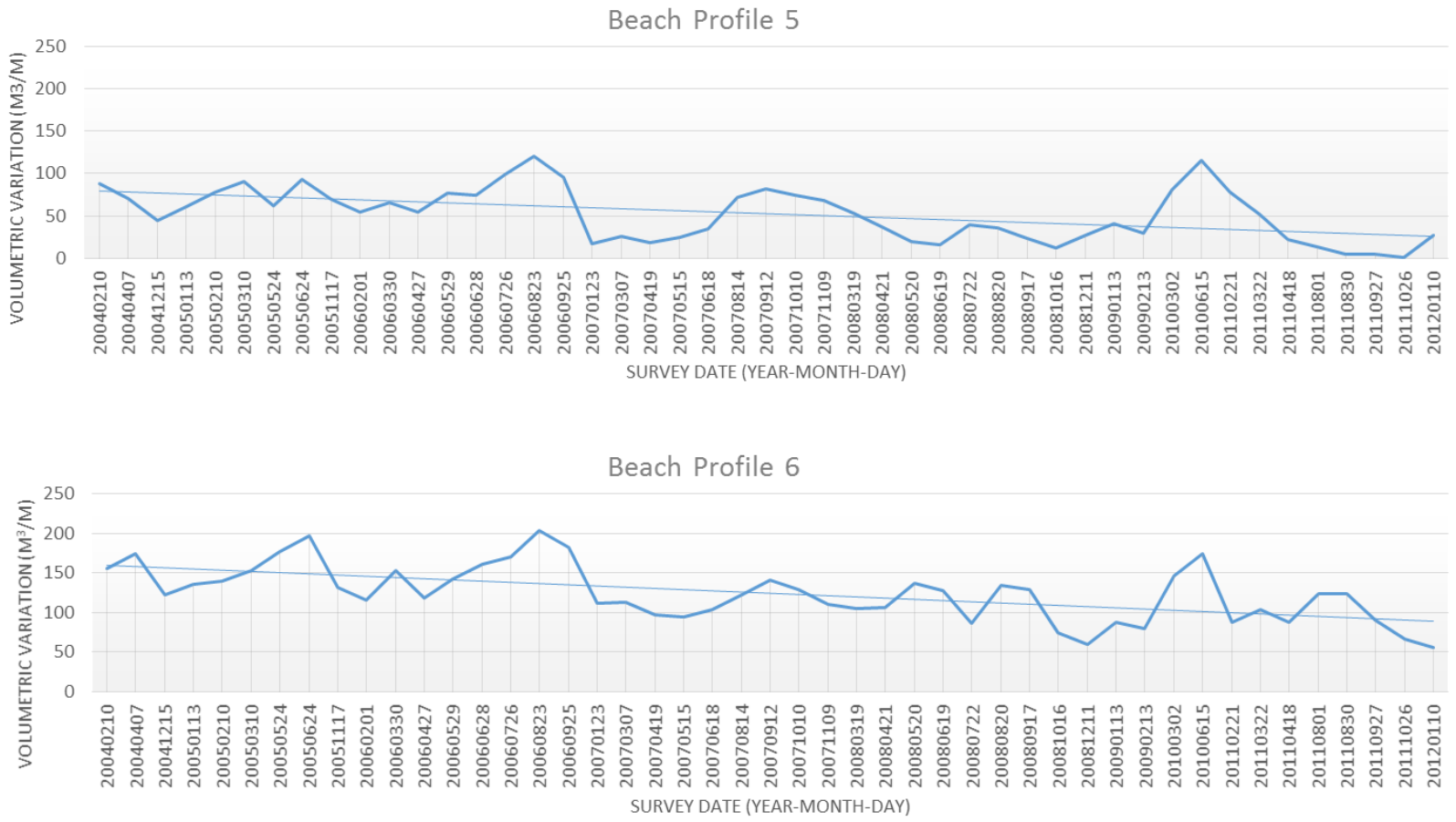

Figure 5.7 (Cont.): Beach Profiles volumetric variations during the study period.

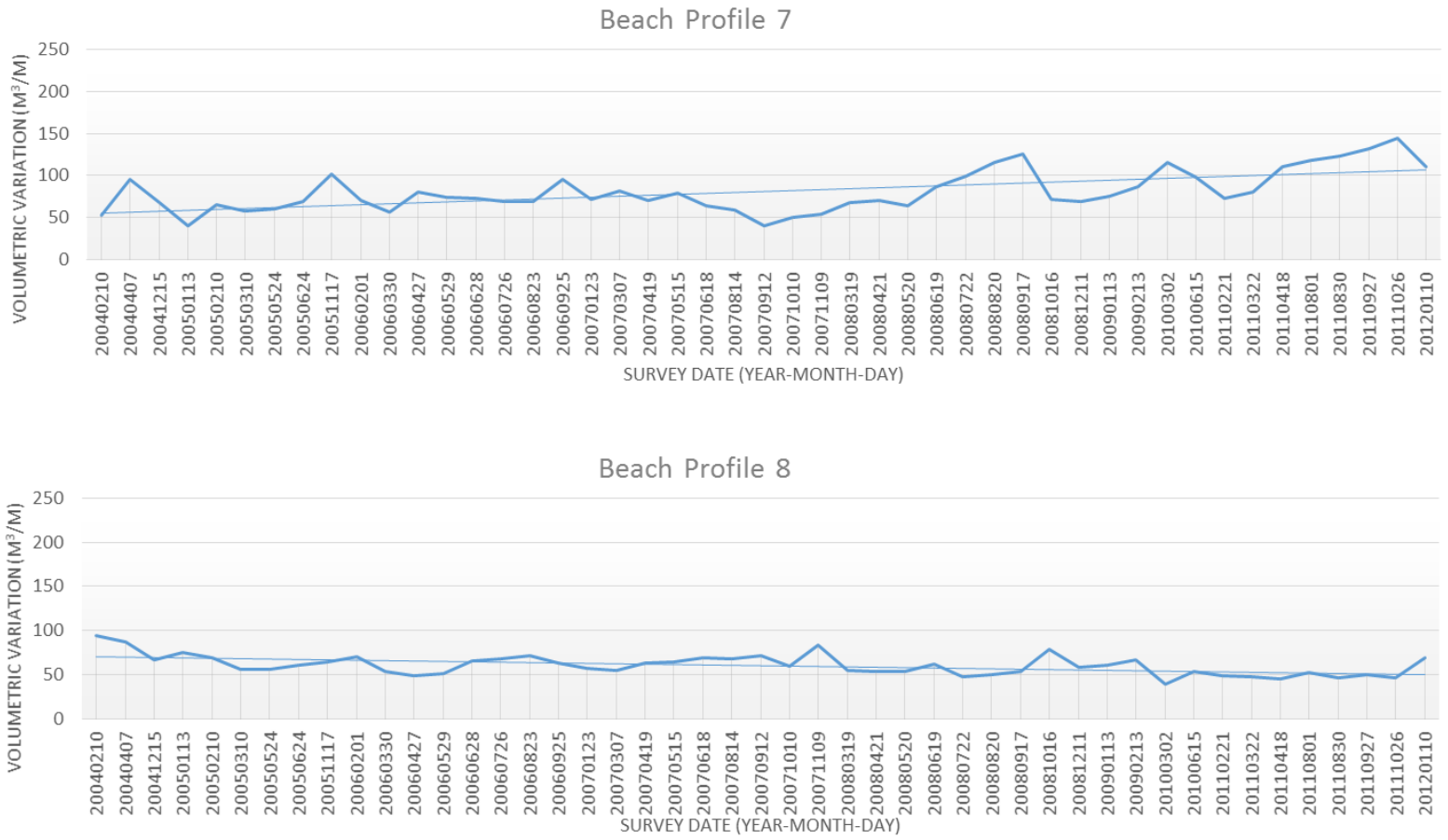

Figure 5.8: Beach Profiles volumetric variations during the study period.

For the profile behaviour representation the tool produces an image for each profile, and another image containing the first and last profile of the study. The following figures are the result of the overlap of profiles 6 and 7 (Figures 5.9 and 5.10), profiles that showed greater erosion and greater accumulation, respectively.

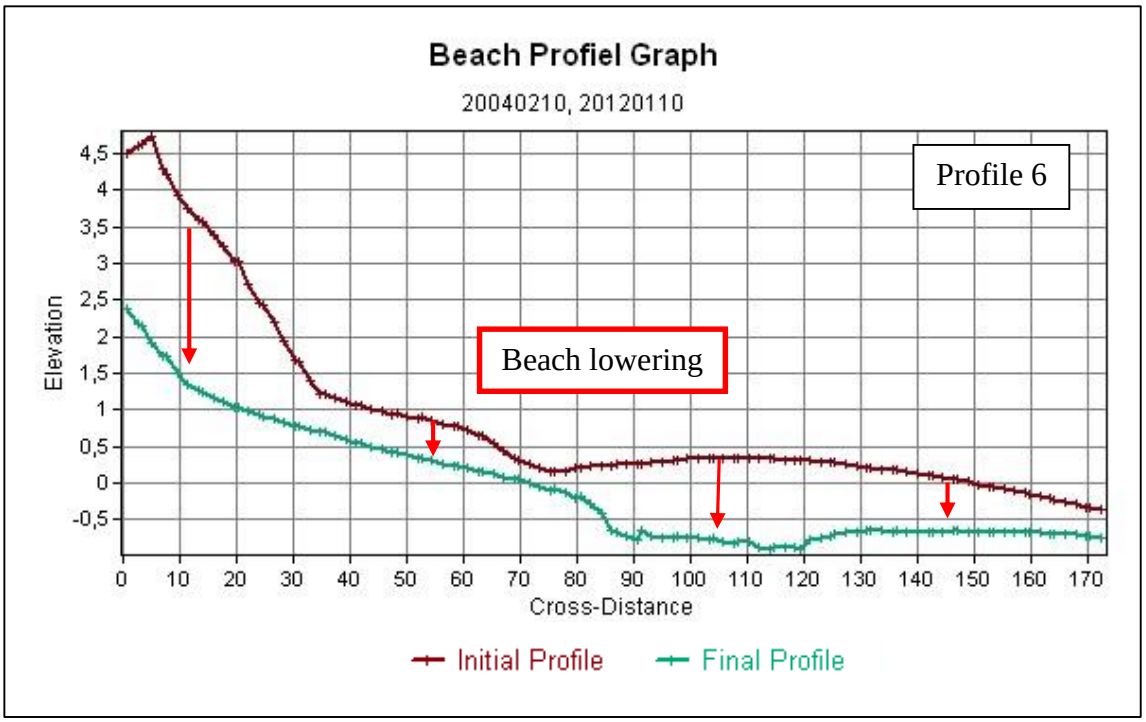

Figure 5.9: BeachPROG result with beach profile graph overlapping of profile 6 from 2004 and 2012.

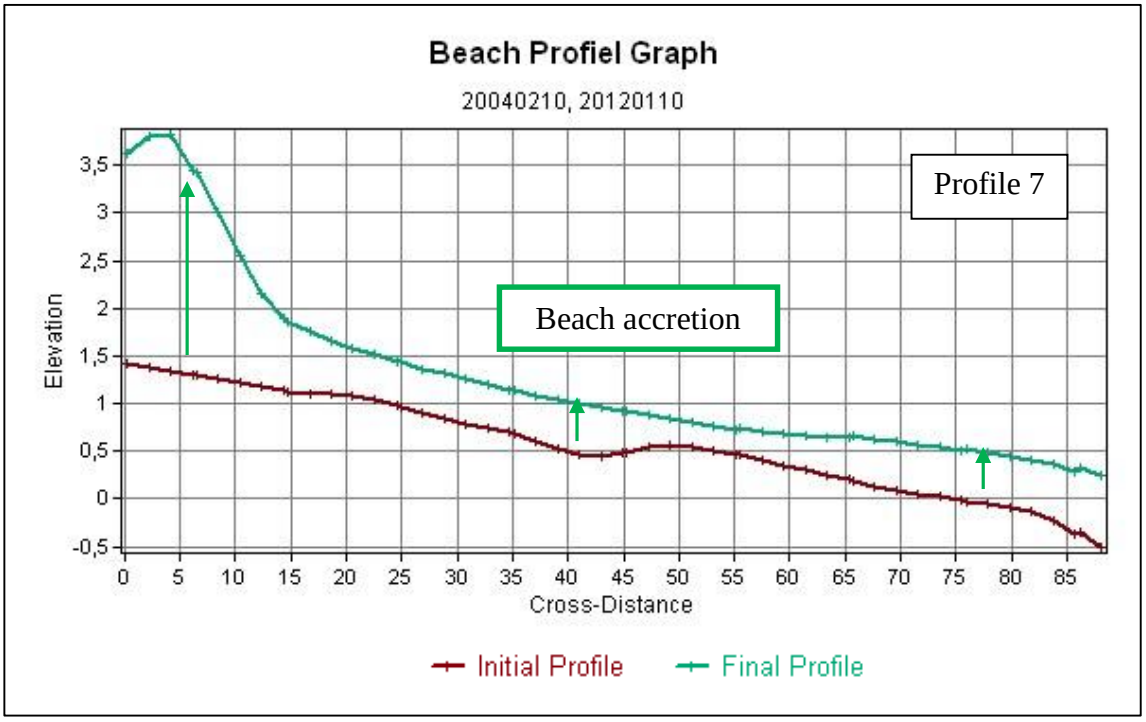

Figure 5.10: BeachPROG result with beach profile graph overlapping of profile 7 from 2004 and 2012.

5.2 DRIVING FACTORS AND BEACH VOLUMETRIC VARIABILITY

5.2.1 Hso interactions

5.2.1.1 Interaction between Hso and beach volumetric behaviour

Conditions where the beach is exposed to regular sea waves and no change in its angle of attack does not always happen, hindering the identification of agents that force such behaviours. In a perfect condition an inverse relationship exists between these two variables. That is, when the volume of sand increases the wave height decreases, or the opposite. However, such conditions do not always occur, evidencing the intervention of external agents on beach behaviour.

For Five Finger Strand, analyses of the relationship / interaction between wave height and beach volumetric variations were performed using the monthly average of Hso values, based on daily average, a month before the dates of volumetric surveys of the beach.

Five Finger Strand presents both episodes. Through figure 5.11 it is possible to verify that there are periods where the volume variability is inversely proportional to the Hso (marked in green). The green marks correspond to periods of 2004/12, 2005/02, 2005/05, 2005/06, 2005/11, 2006/03, 2006/04, 2006/07, 2006/08, 2006/09, 2007/05, 2007/06, 2008/04, 2008/05, 2008/08, 2008/09, 2009/02, 2010/03, 2011/08, 2011/09/, 2011/10 and 2012/01. The remaining periods do not show this relationship. That is, when volume increases Hso also increases and vice versa.

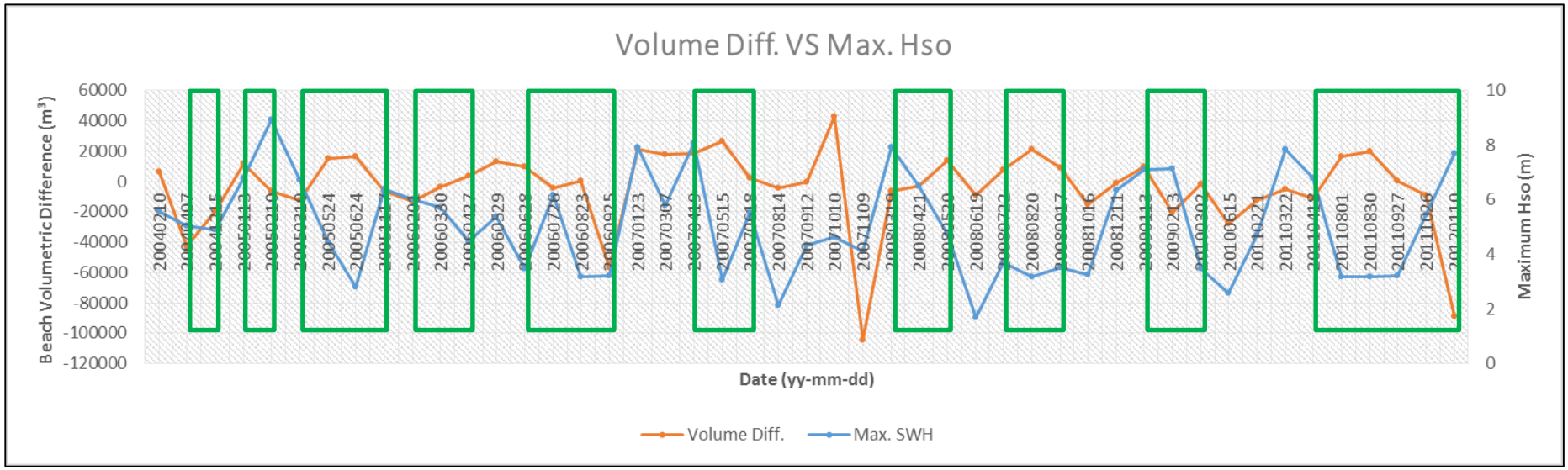

Figure 5.11: Volumetric difference versus maximum Hso variation. Periods where the volume variability trend is inversely proportional to the wave height variability trend are marked in green.

5.2.1.2 Beach behaviour and Hso thresholds

Once the beach showed moments of direct relationship between wave height and beach volumetric variation, as well as moments of inverse relationship, which has evidenced by the intervening of external agents, the existence of relationship between waves direction and recorded heights was then examined.

Thus, the maximum wave height of the daily average a month before the month of field surveys was used. The relationship between a certain level of Hso and the beach behaviour can be checked through the figures 5.12 and 28 below. It is possible to verify that Hso shows generally lower values than those presented in Figure 5.13, ranging between 3 and 6 m.

In contrast, figure 5.13, which corresponds to periods in which there is no inverse correlation between beach volume and wave action, Hso generally lie between 2 and 7 m.

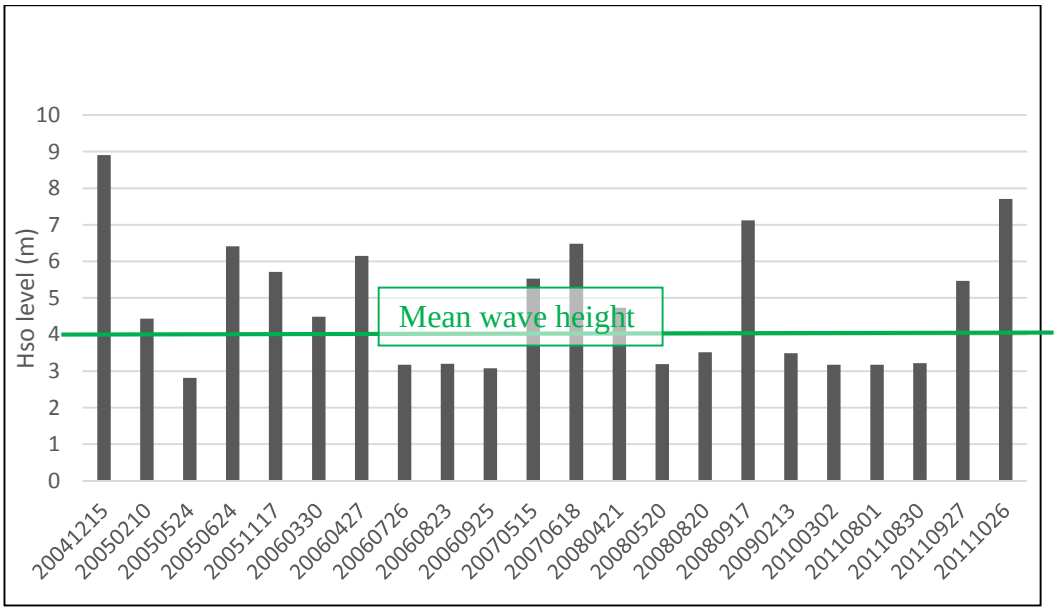

Figure 5.12: Maximum wave height of the daily average a month before the month of field surveys. These periods correspond to the months in which occurred inverse relationship between wave height and beach behaviour. Data are generally between 3 and 6 m.

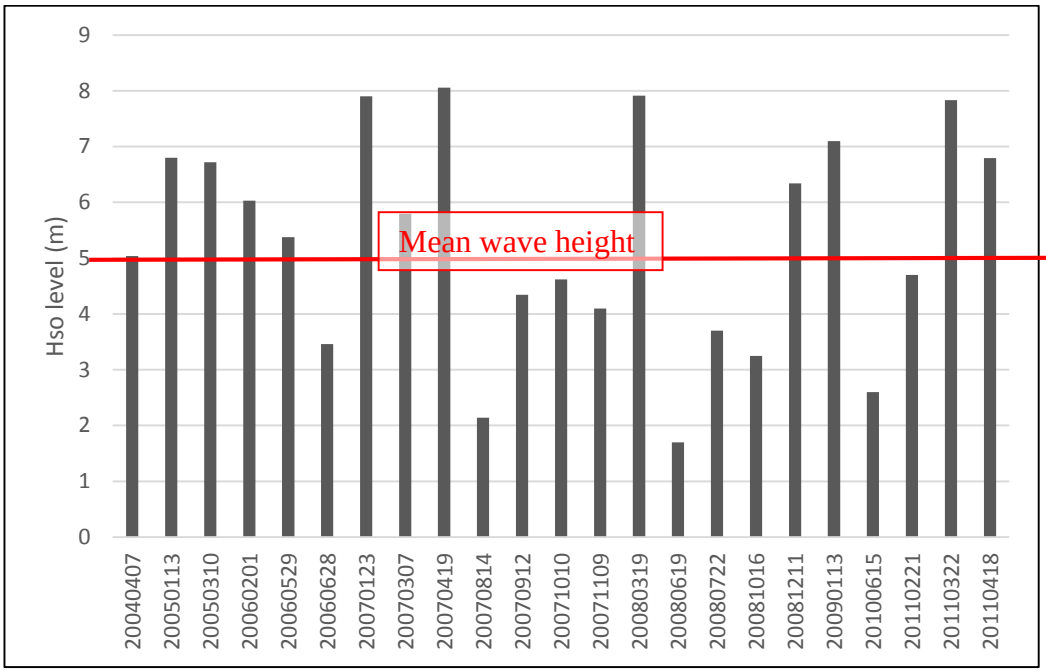

Figure 5.13: Maximum wave height of the daily average a month before the month of field surveys. These periods correspond to the months in which occurred direct relationship between wave height and beach behaviour Data are generally between 2 and 7 m.

5.2.1.3 Relationship between Hso and beach profile behaviour

The relationship between beach profile volume and Hso for each profile was quantified using a least squares regression applied to each profile. According to Almeida et al., (2011), the best statistical method to correlate these two variables, taking into account the type of relationship being examined, the dependence / independence between variables and the type of relationship between them, is the linear regression..

Linear regression is a method for estimating the conditional (expected value) Y of a variable, given the values of some other variable X. In other words, these relationships essentially predict the beach profile volumetric behaviour in terms of different wave conditions. Figure 5.14 indicates a weak correlation between the two variables. The resulting relationships are:

Profile 1 = 0,0725

Profile 2 = 0,0055

Profile 3 = 0,0711

Profile 4 = 0.0512

Profile 5 = 0,0142

Profile 6 = 0,1442

Profile 7 = 0,0683

Profile 8 = 0,0432

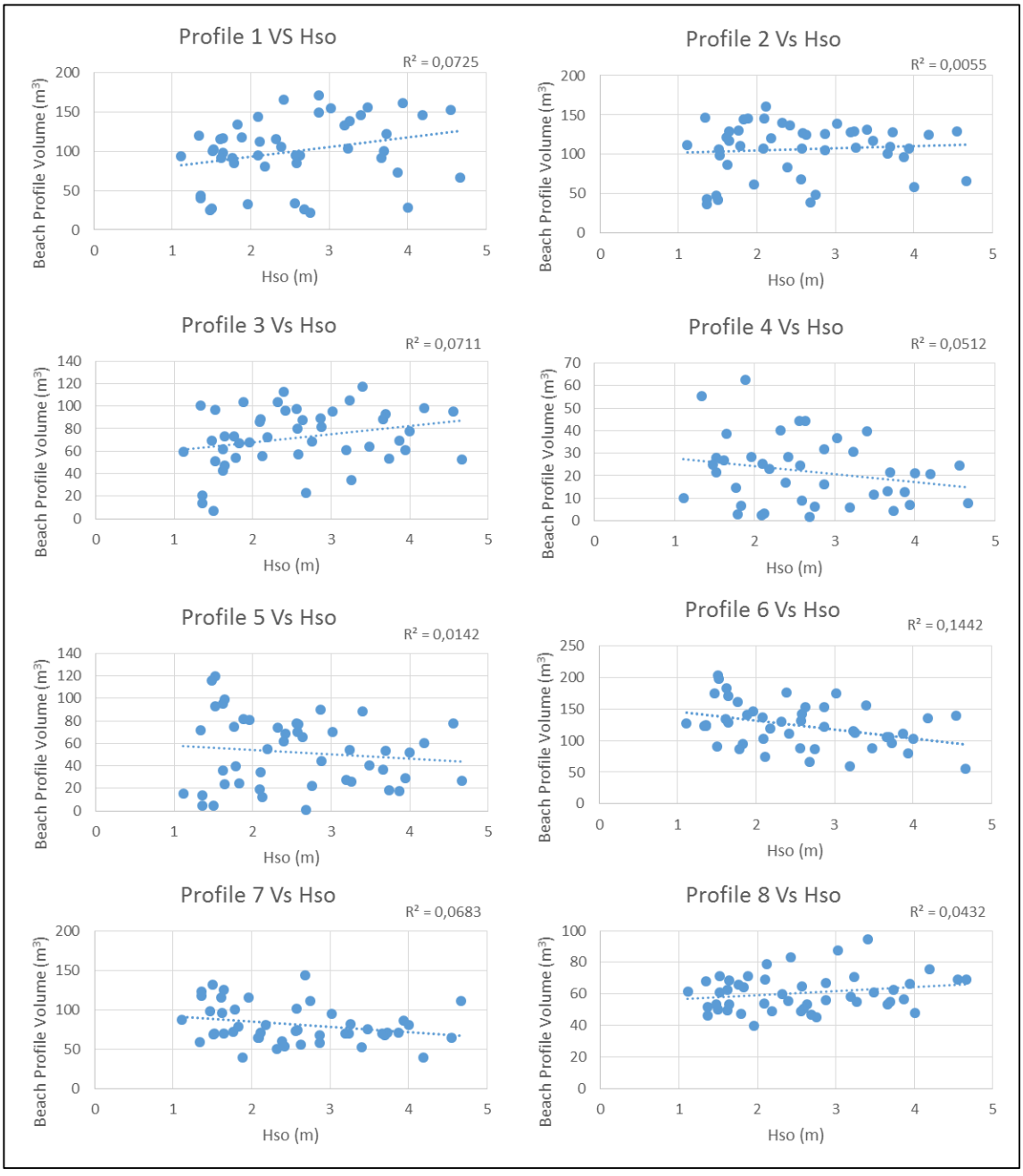

Figure 5.14: Linear regression between beach profiles volumes and Hso.

5.2.2 Channel effects

Highlighting the relationship between the tidal inlet and the adjacent beach morphodynamics, it was made a collection of relevant literature information. Several studies conducted analyses to historical data in order to identify this relationship. The available information contains a number of indicators of geomorphic change over the past 180 years. In a chronological order:

1834 and 1907 - Change in position in the ebb channel from northwesterly to southerly through map observations(O'Connor et al., 2011);

1952 - The inlet channel was in the south, but an abandoned ebb delta in a northwesterly position suggested that the channel had recently moved from north to south (O'Connor et al., 2011);

1977 and 1982 (Figure 5.15) - The ebb channel was located in the south of the embayment and the ebb delta was present at its terminus. The barrier beach maintained a concave, swash-aligned planform and the beach was wide and sandy with a bar near the low tide level. An extensive foredune accumulation, backed by a distinct linear former dune erosion scarp that was well vegetated, was evident. To the south of the inlet channel the rocky coast was fringed by a narrow sandy beach (Cooper et al., 2007 and O'Connor et al., 2011);

1995 – The channel switched once again to the northwest (Cooper et al., 2007 and O'Connor et al., 2011);

2000 Air photographs and field observations showed marked morphological changes compared to the 1977 and 1982 situation (Figure 5.15). The ebb channel extended obliquely across the beach towards the northwest to a new ebb delta deposited at its terminus. Sand from the southern ebb delta had accumulated against the rocky southern margin of the bay, building a wide intertidal beach against the rocky bay margin. In the north, the barrier beach became depleted of sand, exposing patches of the underlying gravel. The foredunes and the frontal margin of the fixed dunes were deeply eroded (Cooper et al., 2007);

2001 to 2004 - The northern ebb delta began to be reworked by wave action into a series of landward-migrating bars on the intertidal and subtidal beach (Cooper et al., 2007);

February, 2004 - The beach had assumed an overall planar sandy form, covering the formerly exposed gravel (Cooper et al., 2007);

2008 - The channel was in the north and the beach showed signs of stability and the subtidal bars appeared to be increasing in size with small amounts of sediment migrating onshore periodically (O'Connor et al., 2011).

Figure 5.15: Channel position variability throughout the years. Font: Cooper et al., (2007). Explanations for each date can be found at the text.

In summary, the tidal inlet suffered cyclical variations in position. From maps of 1834, 1907 and 1952, the ebb channel showed signs that had recently moved to south. That is, the channel changed three times its position between the periods 1834 and 1952. Then, since 1952, the beach suffered an accretion period, and the beach was wide and sandy with a bar near the low tide level. An extensive foredune accumulation was also evident. In 1995, the channel switched once again to the northwest. Five years later it was clearly evident the morphological changes in the behaviour of both beach and channel. A wide

intertidal beach was built against the southern bay margin. In the north, the beach became depleted of sand, exposing the underlying gravel. The foredunes and the frontal margin of the fixed dunes were deeply eroded. In 2004, the beach started showing signs of stability, once it had assumed an overall planar sandy form, covering the formerly exposed gravel. In 2008 the beach was completely stable. The subtidal bars appeared to be increasing and small amounts of sediment migrating onshore periodically.

5.2.3 Wave direction

The behaviour of the beach mentioned above at point 5.2.1 may be in response to the sea waves' direction of actuation. To evaluate the relationship between these two parameters two graphs were created, one with the directions of the waves recorded in "green" periods and the other with the remaining directions.

Figure 5.16a, which represents the direction of the waves within the green periods, shows different angles of incidence. Despite angle variation from SWS to WNW, a greater number of records are between W and WNW directions.

The opposite is also possible to check with figure 5.16b. That is, despite it varies between SSW and WNW direction, the greater angle of incidence for these periods was between SW and W.

It is therefore possible to see that waves from W-WNW seem to have an inverse response between wave height and beach volume change while waves from WSW do not seem to have such reaction.

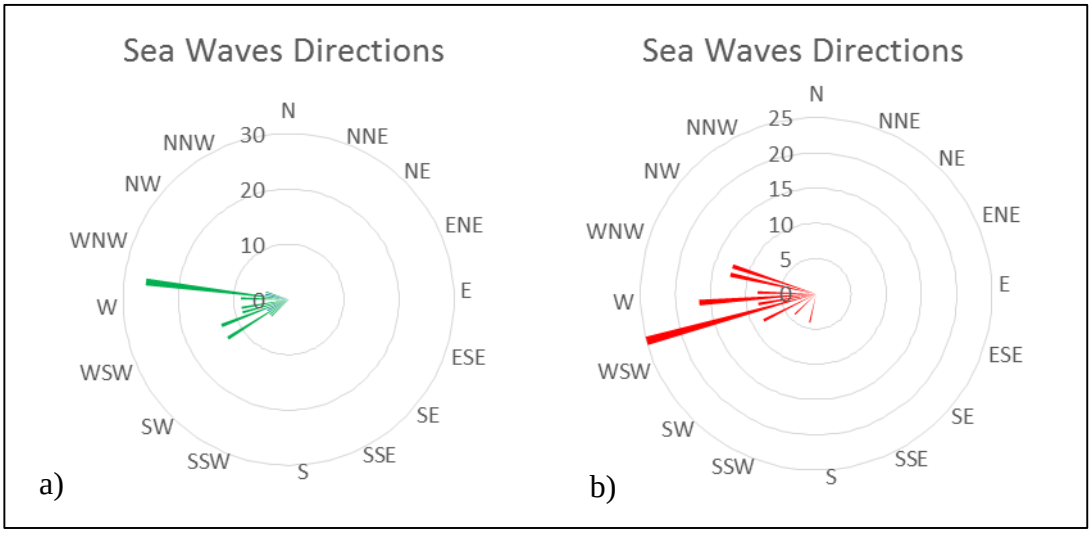

Figure 5.16: Sea waves directions from "green periods" (a) and remaining ones (b).

5.2.4 Occurrence of lateral sediment transport

In open beaches, some of the sediment is transferred alongshore from one profile to another, so that one can react negatively and one positively to the wave's actuation. That is, exists sediment transference from some profiles to others. Such variations are highly dependent on the direction of wave's action, for the occurrence of erosion. For the existence of accumulation processes, this may be related to shoreline direction, natural or artificial obstacles, interaction of external forcing factors, etc.).

To analyse the existence of such situations, the wave records were divided into two angles of incidence. Since the beach is positioned S-N, this division was made between S-W-N. So, one group contains directions from S to W and the other one from W to N. Subsequently, for each wave direction group(S-W and W-N), the volumetric difference between months / years was calculated (02/2004 - 01/2004). The sum of these values was used to verify the existence of alongshore sediment transference (Figures 5.17 and 5.18). This process was repeated for the eight profiles.

The behaviour of beach profiles was then analysed. The group containing the incidence angle between W and N is composed of periods of 2004/12, 2005/02, 2005/06, 2006/05, 2006/09, 2007/04, 2007/06, 2007/08, 2007/09, 2007/10, 2008/04, 2008/11, 2010/06,

2011/02, 2011/08 and 2012/01. All other records present incidence angles between W and S.

Through the figures 5.17 and 5.18 it is possible to verify that the lateral sediment transference has an inverse correlation relative to the wave's action. That is, waves with angles of incidence from NW quadrant provide sediment transference to the north side (accumulation at north and erosion at south of the beach), and SW waves provide sediment transference to the south side (accumulation at south and erosion at north).

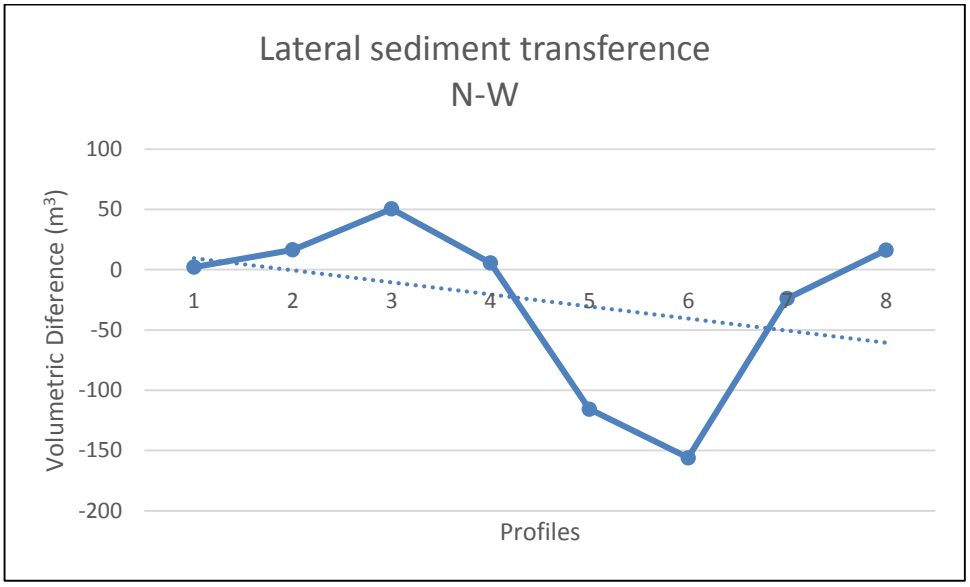

Figure 5.17: Lateral sediment transport between profiles with incidence wave angle from NW quadrant. The volume difference is related to the sum of all volumetric difference values for periods of 2004/12, 2005/02, 2005/06, 2006/05, 2006/09, 2007/04, 2007/06, 2007/08, 2007/09, 2007/10, 2008/04, 2008/11, 2010/06, 2011/02, 2011/08 and 2012/01 for each profile.

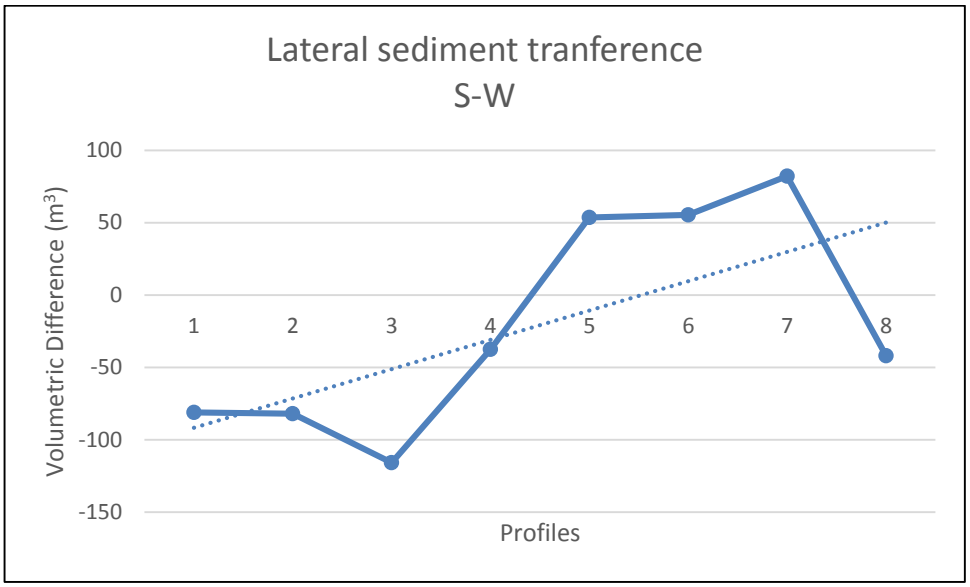

Figure 5.18: Lateral sediment transport between profiles with incidence wave angle from S to W quadrant. The volume difference is related to the sum of all volumetric difference values for all other periods not included in the figure 5.17.

CHAPTER 6

6 DISCUSSION

6.1 BeachPROG TOOL FUNCTIONALITY

The BeachPROG tool proved to be able to integrate and process data in a GIS environment in an easy and convenient way. By owning a set of interconnected processes, it is also possible the addition, removal and modification of existing relations between each process within the tool.

The tool fields needed for running the BeachPROG tool are easy to fill and are properly documented, making the results easily reproducible. However, it is important to know and respect the input formats and know exactly the correspondent output, thus enabling a proper operation / application of the tool. This information can be accessed at the tool's window as well as in the PDF document available within the tool´s folder. For less experienced users with GIS environments, the tool shows in a simple and intuitive way the achieved results of the data acquired at Five Finger Strand.

However, the delay in obtaining results from the tool is one of problems verified. That is, while simplifying the work of the users by decreasing the number of processes required to achieve the results, high interconnection between processes makes its functionality extremely slow and requires an extra effort from the computer.

It is also important to mention the fact that this tool requires the use of ESRI ArcGIS® software and their extensions, presenting difficulties for use by less experienced users as well as all conditions involving the use of a closed source software.

Another downside of using the tool is that it does not allow graphical interaction of input data, forcing users an early selection and verification of data.

In order to extend and improve its applicability in the study of the morphodynamics of beaches, the tool needs to be adapted with the addition of new processes. However, for this study, the tool proved to be perfectly able to assist in studies of the morphodynamics of Five Finger Strand. Thus, the BeachPROG tool reveals to be a tool with great potential to help the scientific community as well as to be a tool with the potential to assist in intervention of coastal managers.

6.2 VOLUMETRIC CHANGES AND WAVE INFLUENCE

The occurrence of erosion at Five Finger Strand is evident. However, understanding the behaviour of the beach over the years and identifying the forcing agents and predicting their behaviour, is fairly difficult. As an initial premise, Five Finger Strand (as other beaches worldwide) experience high temporal variability in erosion and accretion because it suffers the action of wave swash and backwash, tides, climate, and sea-level (Rodriguez, Rodriguez, & Fegley, 2012). Other driving factors are the distance between headlands, bay shape, grain size, nearshore slope (Klein & Menezes, 2001), and tidal inlet influence (O'Connor et al., 2011). These are very generic driving mechanisms that must be studied in particular for each coastal area to define what are the most relevant mechanisms to justify the observed evolutionary behaviour.

The beach behaviour obtained here is quite complex and do not complies with all interactions described above. Briefly, it is possible to verify that the beach evolution is dominated by erosion periods (Figure 5.2), as accretions following each successive erosion were not sufficient to regain the position of earlier shorelines. This variability is an established trend over 8 years and reflects a sedimentary loss, probably associated with a lower sediment source to the region or greater loss in the system (e.g. to the submerse zone). However, as the evaluation of the total sediment budget was not performed in this Dissertation, it is not possible to indicate the effective reason that leads to this sedimentary loss. The results obtained during this study support this conclusion, and are referenced below.

Despite this erosive trend, it has not occurred evenly along the beach. It was found by qualitative and quantitative methods that the northern part of the beach seems to be

retreating toward the dune. Instead, the southern area showed sediment movement toward the sea. This trend causes slight rotation in the direction of beach orientation, exposing the southern area to a greater wave's incidence. Results obtained through the analysis of beach profiles also support this analysis. Results of volumetric variations for each profile indicate that all the profiles have been eroded, with the exception of profile 7 (Figure 5.5, 5.6, 5.7 and 5.8).

Equally, the initial and final profiles overlap observation (2004 and 2012), provided that the landward areas suffered greater variation, both positive (profile 7), and negative (the remainer of profiles). The areas between the ~ 100 and ~ 130 m seaward also showed relatively significant variations. In the remaining parts of profiles, variation was almost parallel to the initial profile's shape (Figure 5.9 and 5.10).

Consequently, it was found a pattern of beach morphological variation: generalized beach lowering by erosion and inland migration throughout the northern sector and from profile 1 to 6; and enlargement of beach in the south, especially in profile 7, which leads to a beach reconfiguration.

The channel can also be an important external force influencing beach behaviour, which contribute to beach volume variation of one month to another. Cooper et al., (2004, 2007) and O'Connor et al., (2007) verified that when the channel is in the northwestern position, which occurred during the entire study period, the ebb channel builds a new ebb tidal delta at its terminus, drawing sand from the adjacent beach. This leads to lowering of the beach and enables waves to propagate landward and erode the base of the dune. This eroded sand is transferred to the growing northern ebb tidal delta. The southern ebb tidal delta is simultaneously abandoned and is reworked by wave action to nourish the pocket beaches on the southern margin of the embayment.

Qualitative relationships can be identified with the channel interaction. From the literature review mentioned above, results by Cooper et al., (2004, 2007) and O'Connor et al., (2007), revealed the increase occurrence of subtidal bars in 2008. From results of this Dissertation, and now relating the evolution of the beach at a smaller scale (months), the identification of all periods with inverse relationship between wave action and beach volumetric variability can also be related to channel's interactivity. Accordingly, periods with inverse relationship between wave action and beach volumetric variability (Figure

5.16) correspond mainly to the direction of wave propagation between WNW and W. The remaining periods occurred with directions between SW and W (Figure 5.16). Knowing that waves from WNW -W provide erosion when the sea waves are greater, and accumulation when the wave propagation is smaller, angles incidence between SW and W appears to suffer interactions with other forcers. In this case, the channel effect seems to co-operate with this waves' angle. That is, when the wave height increases, coupled with the effect of the channel, the beach erodes. On the other hand, when the wave height decreases, the channel effect prevents the beach recovery and so continued erosion or stability exists. It is important to mention that the channel is not effective to attenuate wave's energy due to the depth of the channel while the subtidal bars are effective in mitigating this energy.

More associations can be made with the channel actuation. Such is the case of wave's incidence directions. Results point to an inverse relationship between angle of wave's incidence and direction of lateral sediment transport - sediment exchange between profiles. For waves from NW, sediment appears to move northward. The erosion occurred in the southern beach may be related to the northern headland, which refract the wave, reaching the southern part of the beach. Another possible explanation is the dissipation effect caused by the sand bars which serves to protect the northside of the beach. Waves from SW cause similar effects to the ones provided by the channel. That is, the occurrence of lateral sediment transport to the south. This occurrence reinforces the fact that the waves from the SW quadrant undergo a strong interaction with the channel.

It is also possible to observe that these two groups have different wave heights. While almost half of the periods marked in green occurred with heights below 4 meters, more than half of the remaining periods were subject to wave's height with more than 5 meters. I.e., waves from NW-W and height below 4 meters provided the occurrence of crosshore exchanges. This reveals that beach recovery mainly depends on the regime of wave propagation and that beach erosion suffers the action of other factors. These results can also justify some of the behaviour of alongshore sediment transport.

It becomes clear that interaction between waves and beach exists. Also, the effect of the channel seems to significantly influence both the wave action and the behaviour of the beach. It is also possible to identify a general pattern in this behaviour. However,

quantifying and predicting these interactions is still extremely difficult and cannot be made based on the general results obtained here. Cooper et al., (2004); Jackson et al., (2005) and Backstrom et al., (2009) also verified that even with a storm of high enough magnitude to cause morphological change, other factors produce potentially important differences in coastal response patterns. Such is the case with the high energy swell that arrives fully refracted at the shoreline, where an increase in swell size may not necessarily create a change in wave energy dispersal patterns; the dissipative morphodynamic beach domain, where wave energy is dissipated across the shoreface during increased swell regimes and is unlikely to generate an excess of energy in the nearshore beach; or the mesotidal range felt at Five Finger Strand, where there is a long tidal interval during which short-lived storms will not coincide with such levels, causing a reduced occurrence of elevated water levels that exceed normal tidal high water levels. Similarly, O' Connor et al., (2009) have concluded that the erosion at this site is part of a longer erosion/accretion cycle.

More studies should be conducted in order to identify and understand all the processes that operate and influence the morphology of Five Finger Strand. Besides closely monitoring the morphological beach evolution, with decreased temporal spacing between field surveys, which can currently be done with refuse to satellite images; a detailed study of the main conditions of sedimentary transference should be performed, thus observing the patterns of refraction and energy dissipation relative to sediment transfer. It should also be estimated regional sediment budget, which includes the submerged bars and estuary, thereby realizing the sediment loss, its cause and location of the transferred sediment.

CHAPTER 7

7 CONCLUSION

The knowledge of environmental impacts that influence the beach behaviour at Five Finger Strand requires an understanding of the way terrestrial and marine processes operate and interact with each other. This requires high-frequency surveys that for reasons of unsustainability, degrades severely the measurement accuracy as sampling frequency decreases. Also, the spatial distance between sampling profiles also present difficulties in our understanding of these interactions.

The method used here to understand the beach behaviour consists of quantifying the beach volumetric variation for each survey period, the analysis of the hydrodynamic forces caused by waves and then examination of the correlation or a statistical analysis derived from an explicit comparison of the beach volume and hydrodynamic data series. Because of the complexity of survey data, and to facilitate its manipulation, a GIS tool was created – BeachPROG that automates the intermediate steps to obtain beach volumes and profiles.

This tool revealed in a general way good results, as the data automation, visualization, spatial consultation, and spatial analysis can be accessed in a much more intuitive way. It is equally important to mention that this tool can serve as a methodological base for other investigations, presenting a fully commented, easy script structure that enables further modifications and / or script accretions. Contrary, despite being easy to work and intuitive, it does not allow graphical interaction of input data, forcing users an early selection and verification of data. Also, it is important to know and respect the input formats and know exactly the corresponding output, thus enabling an accurate operation / application of the tool. Another difficulty verified with this tool was the delay in obtaining results. The high interconnection between processes is the cause of this delay in processing all data.

The tool proved to be perfectly capable of assisting in the examination of Five Finger Strand morphodynamics. For that reason, the BeachPROG tool revealed to have great potential in helping the scientific community as well as assisting in the intervention of coastal managers.

With volumetric data as a starting point, comparisons with hydrological data were performed. From what has been discussed throughout this Dissertation, as well as based on previous papers mentioned throughout this work, it can be seen that there are two types of beach behaviours:

- Short term evolution, which encompasses the response of the beach to the action of storms:
  - It is easily identifiable a link between the existence of beach behaviour with the direction of wave action. Waves from the NW quadrant has an inversely proportional relation to the beach volumetric variation: when one increases the other one decreases and vice versa.
  - Similarly, for waves of the same quadrant, there is an alongshore sediment transfer from south to north, which can be explained by the existence of the northern headland that protects the northern beach, while it causes a rotation in the direction of the wave, causing direct interaction with the southern beach. The sand bars also provide protection from direct wave actuation.
  - Waves from the SW quadrant showed to interact with the beach quite differently. There is clear interaction of channel with sediment transport from north to south, due to sediment transfer from the beach to the ebb tidal delta (in the northern beach), and sediment transference from the abandoned ebb tidal delta to the south beach (accumulation in the southern area), that causes slight rotation in the direction of beach orientation and exposes the southern area to a greater wave's incidence.
- Long term beach evolution (years), evidenced through two distinct behaviours:
  - Sediment loss over the years, with an average of $\approx 2000\ m^3$/year. This loss seems to be directly linked to the performance of the ebb tidal channel with sediment transfer from the beach to the ebb tidal delta / sand bars. This erosive behaviour seems to be linked to the channel's position, since

the north position causes erosive behaviour and south a cumulative behaviour. Note that the channel was north throughout the period under study.

- Furthermore, the existence of sediment movement toward the base of the dune in the north, and towards the sea in the south, which causes slight rotation in the direction of beach orientation, exposes the southern area to a greater wave's incidence.

Full detailed comprehension of how interaction take place between the beach, the prevailing hydrological force and the existence of other influential agents cannot be revealed within the scope of this Dissertation. Further studies should be conducted in order to identify and understand all the processes that operate and influence the morphology of Five Finger Strand. Besides closely monitoring the morphological beach evolution, a detailed study of the main conditions of sedimentary transference should be performed. It should also be estimated regional sediment budget, which includes the submerged bars and estuary.

8 LITERATURE CITED

Aagaard, T., Kroon, A., Andersen, S., Sørensen, R. M., Quartel, S., & Vinther, N. (2005). Intertidal beach change during storm conditions; Egmond, The Netherlands. *Marine Geology*, *218*(1-4), 65–80.

Algarni, D. A., & El hassan, I. M. (2001). Comparison of thin plate spline, polynomial, C—function and Shepard's interpolation techniques with GPS-derived DEM. *International Journal of Applied Earth Observation and Geoinformation*, *3*(2), 155–161.

Allen, T. R., Oertel, G. F., & Gares, P. A. (2012). Mapping coastal morphodynamics with geospatial techniques, Cape Henry, Virginia, USA. *Geomorphology*, *137*(1), 138–149.

Almeida, L. P., Ferreira, Ó., & Pacheco, a. (2011). Thresholds for morphological changes on an exposed sandy beach as a function of wave height. *Earth Surface Processes and Landforms*, *36*(4), 523–532.

Andrews, B., Gares, P. A., & Colby, J. D. (2002). Techniques for GIS modeling of coastal dunes. *Geomorphology*, *48*(1-3), 289–308.

Anfuso, G. (2005). Sediment-activation depth values for gentle and steep beaches. *Marine Geology*, *220*(1-4), 101–112.

Anthony, E. J., & Orford, J. D. (2002). Between Wave- and Tide-Dominated Coasts : the Middle Ground Revisited. *Journal of Coastal Research*, *15*(36), 8–15.

Backstrom, J. T., Jackson, D. W. T., & Cooper, J. a G. (2009). Shoreface morphodynamics of a high-energy, steep and geologically constrained shoreline segment in Northern Ireland. *Marine Geology*, *257*(1-4), 94–106.

Balsillie, J. H. (1986). Beach and Coast Erosion Due to Extreme Event Impact. *Shore and Beach*, *54*(4), 22–37.

Benavente, J., Del Río, L., Afunso, G., Gracia, F. J., & Reyes, J. L. (2002). Utility of Morphodynamic Characterisation in the Prediction of Beach Damage by Storms. *Journal of Coastal Research*, (36), 56–64.

Benavente, J., Gracia, F. J., & López-Aguayo, F. (2000). Empirical model of morphodynamic beachface behaviour for low-energy mesotidal environments. *Marine Geology*, *167*(3-4), 375–390.

Birkemeier, W. A., Asce, A. M., Nicholls, R. J., & Lee, G.-H. (1999). Storms, Storm Groups and Nearshore Morphologic Change. *Coastal Sediments*, 1109–1123.

Bishop, T. F. A., McBratney, A. B., & Whelan, B. M. (2001). Measuring the quality of digital soil maps using information criteria. *Geoderma*, *103*(1), 95–111.

Bossak, B. B. H., Morton, R. A., & Sallenger, A. H. (2005). *A GIS-Based Information System for Predicting Impacts from Coastal Storms – The Coastal Impact Assessment Tool (CIAT), Version 1 . 0 , User ' s Manual*.

Butler, H. (2005). *A Guide to the Python Universe for ESRI Users*. *ArcUser* (pp. 34–37).

Carter, R. W. G. (1975). Recent Changes in the Coastal Geomorphology of the Magilligan Foreland , Co . Londonderry. *Chemical Science*, *75*(1975), 469–497.

Carter, R. W. G. (1982). Recent Variations in Sea-Level on the North and East Coasts of Ireland and Associated Shoreline Response Author (s): R . W . G . Carter Reviewed work (s): Source : Proceedings of the Royal Irish Academy . Section B : Biological , Geological , and Publ. *Chemical Science*, *82B*, 177–187.

Carter, R.W.G., 1988, Coastal Environments—An Introduction to the Physical, Ecological and Cultural Systems of Coastlines: London, Academic Press, 617 p. In: Backstrom, J. T., Jackson, D. W. T., & Cooper, J. a G. (2009). Shoreface morphodynamics of a high-energy, steep and geologically constrained shoreline segment in Northern Ireland. *Marine Geology*, *257*(1-4), 94–106.

Bernabeu, A. M., Medina, R., & Vidal, C. (2003). A morphological model of the beach profile integrating wave and tidal influences. *Marine Geology*, *197*(1-4), 95–116.

Storms, J. E. A., Weltje, G. J., Dijke, J. J. Van, Geel, C. R., & Kroonenberg, S. B. (2002). Process-Response Modeling of Wave-Dominated Coastal Systems:Simulating Evolution and Stratigraphy on Geological Timescales. *Journal of Sedimentary Research*, *72*(2), 226–239.

Carter, R. W. G., & Balsillie, J. H. (1983). A Note on the Amount of Wave Energy Transmitted Over Nearshore Sand Bars. *Earth Surface Processes and Landforms*, *8*, 213–222.

Cooper, J. A. G., Jackson, D. W. T., Navas, F., McKenna, J., & Malvarez, G. (2004). Identifying storm impacts on an embayed, high-energy coastline: Examples from western Ireland. *Marine Geology*, *210*(1-4), 261–280.

Cooper, J. A. G., & Mckenna, J. (2008). Working with natural processes: the challenge for coastal protection strategies. *The Geographical Journal*, *174*(4), 315–331.

Cooper, J. A. G., McKenna, J., Jackson, D. W. T., & O'Connor, M. (2007). Mesoscale coastal behavior related to morphological self-adjustment. *Geology*, *35*(1), 187–190.

Cooper, J. A. G., & Pilkey, O. H. (2004). Longshore Drift: Trapped In An Expected Universe. *Journal of Coastal Research*, *74*(5), 599–606.

Davis, R. A., & Hayes, M. O. (1984). What is a Wave-Dominated Coast? *Marine Geology*, *60*, 313–329.

Dean, R. G. (1991). Equilibrium Beach Profiles: Characteristics and Applications. *Journal of Coastal Research*, *7*(1), 53–84.

Dee, D. P., Uppala, S. M., Simmons, a. J., Berrisford, P., Poli, P., Kobayashi, S., … Vitart, F. (2011). The ERA-Interim reanalysis: configuration and performance of the data assimilation system. *Quarterly Journal of the Royal Meteorological Society*, *137*, 553–597.

Desmet, P. J. J. (1997). Effects of interpolation errors on the analysis of DEMs. *Earth Surface Processes and Landforms*, *22*(6), 563–580.

Dobesova, Z. (2011). Programming language Python for data processing. In *2011 International Conference on Electrical and Control Engineering* (pp. 4866–4869).

Duffy, W., & Dickson, S. M. (1995). Using grid and graph to quantify and display shoreline change. Retrieved March 16, 2014, from http://proceedings.esri.com/library/userconf/proc95/to100/p074.html

Erdogan, S. (2009). A comparision of interpolation methods for producing digital elevation models at the field scale. *Earth Surface Processes and Landforms*, *34*(1), 366–376.

ESRI. (2002). *Spatial Analyst Help Documentation. ArcGIS Users' Guide. ESRI Inc.* (p. 563).

Farris, A. S., & List, J. H. (2007). Shoreline Change as a Proxy for Subaerial Beach Volume Change. *Journal of Coastal Research*, *23*(3), 740–748.

Ferreira, Ó. (2005). Storm groups versus extreme single storms: predicted erosion and management consequences. *Journal of Coastal Research*, *42*, 221–227.

Ferreira, Ó. (2006). The role of storm groups in the erosion of sandy coasts. *Earth Surface Processes and Landforms 1058*, *31*, 1058–1060.

Ferreira, Ó., & Alveirinho Dias, J. (2000). Prediction of storm impacts and shoreline retreat induced by hypothetical storms on open coastlines.

Fischer, P. F., & Tate, N. J. (2006). Causes and consequences of error in digital elevation models * Peter F. *Progress in Physical Geography*, *30*(4), 467–489.

Forbes, D. L., Parkes, G. S., Manson, G. K., & Ketch, L. A. (2004). Storms and Shoreline Retreat in the Southern Gulf of St. Lawrence. *Marine Geology*, *210*, 169–204.

Gong, J., Zhllin, L., Zhu, Q., Sui, H., & Zhou, Y. (2000). Effects of Various Factors on the Accuracy of DEMs : An Intensive Experimental Investigation. *Photogrammetric Engineering & Remote Sensing*, *66*(9), 1113–1117.

Harley, M. D., Turner, I. L., Short, A. D., & Ranasinghe, R. (2011). Assessment and integration of conventional, RTK-GPS and image-derived beach survey methods for daily to decadal coastal monitoring. *Coastal Engineering*, *58*(2), 194–205.

Harris, L., Nel, R., & Schoeman, D. (2011). Mapping beach morphodynamics remotely: A novel application tested on South African sandy shores. *Estuarine, Coastal and Shelf Science*, *92*(1), 78–89.

Harris, M., Brock, J., Nayegandhi, A., & Duffy, M. (2005). Extracting Shorelines from NASA Airborne Topographic Lidar-Derived Digital Elevation Models. In *Reston, VA, U.S. Geological Survey Open-file repor* (pp. 2005–1427).

Hashemi, M. R., Ghadampour, Z., & Neill, S. P. (2010). Using an artificial neural network to model seasonal changes in beach profiles. *Ocean Engineering*, *37*(14-15), 1345–1356.

Hengl, T. (2006). Finding the right pixel size. *Computers and Geosciences*, *32*(9), 1283–1298.

Himmelstoss, E. a., FitzGerald, D. M., Rosen, P. S., & Allen, J. R. (2006). Bluff Evolution along Coastal Drumlins: Boston Harbor Islands, Massachusetts. *Journal of Coastal Research*, *225*(September), 1230–1240.

Horta, J., Moura, D., Gabriel, S., & Ferreira, Ó. (2013). Measurement of pocket beach morphology using geographic information technology : the MAPBeach toolbox, (65), 1397–1402.

Jackson, D. W. T., Cooper, J. a G., & Del Rio, L. (2005). Geological control of beach morphodynamic state. *Marine Geology*, *216*(4), 297–314.

Jackson, D. W. T., & Cooper, J. A. G. (2010). Application of the equilibrium planform concept to natural beaches in Northern Ireland. *Coastal Engineering*, *57*(2), 112–123.

Kabdas, M. S., & Tu, U. (2006). The effects of sediment characteristics and wave height on shape-parameter for representing equilibrium beach profiles, *33*, 281–291.

Kaiser, M. F. M., & Frihy, O. E. (2009). Validity of the equilibrium beach profiles: Nile Delta Coastal Zone, Egypt. *Geomorphology*, *107*(1-2), 25–31.

Klein, A. H. da F., & Menezes, J. T. (2001). Beach Morphodynamics and Profile Sequence for a Headland Bay Coast. *Journal of Coastal Research*, *17*(4), 812–835.

Kriebel, D. L., & Dean, R. G. (1993). Convolution Method for Time-Dependent Beach-Profile Response. *Journal of Waterway, Port, Coastal, and Ocean Engeneering*, *119*(2).

Kroon, A., Larson, M., Möller, I., Yokoki, H., Rozynski, G., Cox, J., & Larroude, P. (2008). Statistical analysis of coastal morphological data sets over seasonal to decadal time scales. *Coastal Engineering*, *55*, 581–600.

Kuo, W.-L., Steenhuis, T. S., McCulloch, C. E., Mohler, C. L., Weinstein, D. A., DeGloria, D., & Swaney, D. P. (1999). Effect of grid size on runoff and soil moisture for a variable-source-area hydrology model. *Water Resources Research*, *35*(11), 3419–3428.

Larson, M., Kraus, N. C., & Wise, R. a. (1999). Equilibrium beach profiles under breaking and non-breaking waves. *Coastal Engineering*, *36*(1), 59–85.

Lee, G. H., Nicholls, R. J., & Birkemeier, W. a. (1998). Storm-driven variability of the beach-nearshore profile at Duck, North Carolina, USA, 1981-1991. *Marine Geology*, *148*(3-4), 163–177.

Levoy, F., Anthony, E. J., Monfort, O., & Larsonneur, C. (2000). The morphodynamics of megatidal beaches in Normandy, France. *Marine Geology*, *171*(1-4), 39–59.

Li, Y., Brimicombe, A. J., & Ralphs, M. P. (2000). Spatial data quality and sensitivity analysis in GIS and environmental modelling : the case of coastal oil spills, *24*, 95–108.

Li, Y., Lark, M., & Reeve, D. (2005). Multi-scale variability of beach profiles at Duck: A wavelet analysis. *Coastal Engineering*, *52*(12), 1133–1153.

Li, Z. (1988). On the measure of digital terrain model accuracy. *Photogrammetric Record*, *12*(72), 873–877.

List, J. H., Farris, A. S., & Sullivan, C. (2006). Reversing storm hotspots on sandy beaches: Spatial and temporal characteristics. *Marine Geology*, *226*(3-4), 261–279.

Masselink, G., Auger, N., Russell, P., & O'Hare, T. (2007). Short-term morphological change and sediment dynamics in the intertidal zone of a macrotidal beach. *Sedimentology*, *54*(1), 39–53.

Masselink, G., & Pattiaratchi, C. B. (2001). Seasonal changes in beach morphology along the sheltered coastline of Perth, Western Australia. *Marine Geology*, *172*(3-4), 243–263.

McBratney, A. B. (1998). Some considerations on methods for spatially aggregating and disaggregating soil information. *Nutrient Cycling in Agroecosystems*, *50*, 51–62.

Moore, L. J., & Griggs, G. B. (2002). Long-term cliff retreat and erosion hotspots along the central shores of the Monterey Bay National Marine Sanctuary. *Marine Geology*, *181*(1-3), 265–283.

Morton, R. A. (1979). Temporal and spatial variations in shoreline changes and their implications, examples from the Texas Gulf coast. *Journal of Sedimentary Petrology*, *49*, 1101–1112.

Morton, R. A. (2002). Factors Controlling Storm Impacts on Coastal Barriers and Beaches-A Preliminary Basis for Near Real-Time Forecasting. *Journal of Coastal Research*, *18*(3), 486–501.

Morton, R. a., Clifton, H. E., Buster, N. a., Peterson, R. L., & Gelfenbaum, G. (2007). Forcing of large-scale cycles of coastal change at the entrance to Willapa Bay, Washington. *Marine Geology*, *246*(1), 24–41.

Morton, R. A., Gibeaut, J. C., & Paine, J. G. (1995). Meso-Scale Transfer of Sand During and After Storms:Implications for Prediction of Shoreline Movement. *Marine Geology*, *126*, 161–179.

Muñoz-perez, J. J., & Medina, R. (2010). Comparison of long-, medium- and short-term variations of beach profiles with and without submerged geological control. *Coastal Engineering*, *57*(3), 241–251.

Newe, J., Peters, K., Dette, H.H., 1999. Profile development under storm conditions as a function of the beach face slope. Proc. Coastal Sediments '99. ASCE, New York, pp. 2582–2596. In: Aagaard, T., Kroon, A., Andersen, S., Sørensen, R. M., Quartel, S., & Vinther, N. (2005). Intertidal beach change during storm conditions; Egmond, The Netherlands. *Marine Geology*, *218*(1-4), 65–80.

O' Connor, M. C., Cooper, J. A. G., & McKenna, J. (2009). Integrating Science into Shoreline Management Practice and Policy: an Irish Perspective. *Journal of Coastal Research*, *56*(2), 1267–1270.

O' Connor, M., Cooper, J. A. G., & Jackson, D. W. T. (2007). Morphological Behaviour of Headland-Embayment and Inlet-Associated Beaches , Northwest Ireland. *Journal of Coastal Research*, (50), 626–630.

O'Connor, M. C., Cooper, J. A. G., & Jackson, D. W. T. (2011). Decadal Behavior of Tidal Inlet-Associated Beach Systems, Northwest Ireland, in Relation to Climate Forcing. *Journal of Sedimentary Research*, *81*(1), 38–51.

O'Connor, M. C., Cooper, J. A. G., McKenna, J., & Jackson, D. W. T. (2010). Shoreline management in a policy vacuum: A local authority perspective. *Ocean and Coastal Management*, *53*(12), 769–778.

Olsen, M. J., Young, A. P., & Ashford, S. A. (2012). TopCAT—Topographical Compartment Analysis Tool to analyze seacliff and beach change in GIS. *Computers & Geosciences*, *45*, 284–292.

Pendleton, E. A., Williams, S. J., & Thieler, E. R. (2004). *Coastal vulnerability assessment of assateague island national seashore (asis) to sea-level rise*.

Persson, A., & Andersson, E. (2013). *User guide to ECMWF forecast products* (p. 129).

Rijn, L. C. Van, Walstra, D. J. R., Grasmeijer, B., & Sutherland, J. (2003). The predictability of cross-shore bed evolution of sandy beaches at the time scale of storms and seasons using process-based Profile models, *47*, 295–327.

Rodriguez, A. B., Rodriguez, P. L., & Fegley, S. R. (2012). One-year along-beach variation in the maximum depth of erosion resulting from irregular shoreline morphology. *Marine Geology*, *291-294*, 12–23.

Rodríguez, I., Montoya, I., Sánchez, M. J., & Carreño, F. (2009). Geomorphology Geographic Information Systems applied to Integrated Coastal Zone Management. *Geomorphology*, *107*(1-2), 100–105.

Schoones, J. S., & Theron, K. A. (1995). Evaluation of 10 cross-shore sediment transport/morphological models. *Coastal Engineering*, *25*, 1–41.

Scott, T., Masselink, G., & Russell, P. (2011). Morphodynamic characteristics and classi fi cation of beaches in England and Wales. *Marine Geology*, *286*(1-4), 1–20.

Sénéchal, N., Gouriou, T., Castelle, B., Parisot, J., Capo, S., Bujan, S., & Howa, H. (2009). Geomorphology Morphodynamic response of a meso- to macro-tidal intermediate beach based on a long-term data set. *Geomorphology*, *107*(3-4), 263–274.

Short, A. D. (2006). Australian Beach Systems — Nature and Distribution, *22*(1), 11–27.

Short, A. D., & Trembanis, A. C. (2004). Decadal Scale Patterns in Beach Oscillation and Rotation Narrabeen Beach, Australia - Time Series, PCA and Wavelet Analysis. *Journal of Coastal Research*, *20*(2), 523–532.

Smith, S. L., Holland, D. A., & Longley, P. A. (2005). Quantifying Interpolation Errors in Urban Airborne Laser Scanning Models. *Geographical Analysis*, *37*(2), 200–224.

Smith, S. L., Holland, D., & Langley, P. (2003). Interpreting Interpolation: the Pattern of Interpolation Errors in Digital Surface Models Derived from Laser Scanning Data. *CASA Working Paper*, *66*(Centre for Advanced Spatial Analysis, University College London).

Southgate, H. N. (2008). Data-based forecasting of beach volumes on monthly to yearly timescales. *Coastal Engineering*, *55*(12), 1005–1015.

Stein, A., Riley, J., & Halberg, N. (2001). Issues of scale for environmental indicators. *Agriculture, Ecosystems and Environment*, *87*(2), 215–232.

Storms, J. E. A., Weltje, G. J., Dijke, J. J. Van, Geel, C. R., & Kroonenberg, S. B. (2002). Process-Response Modeling of Wave-Dominated Coastal Systems:Simulating Evolution and Stratigraphy on Geological Timescales. *Journal of Sedimentary Research*, *72*(2), 226–239.

V, W. R., Zhang, K., & Whitman, D. (2007). Hurricane-induced beach change derived from airborne laser measurements near Panama City , Florida, *237*, 191–205.

Van de Graff, J. (1994). Coastal and dune erosin under extreme conditions. *Journal Of Coastal Research*, (12), 253–262.

Vellinga, P., & Klein, R. J. T. (1993). Climate change, sea level rise and Integrated Coastal Zone Management: an IPCC approach. *Ocean & Coastal Management*, *21*(1-3), 245–268.

Vieux, B. E., & Needham, S. (1993). Nonpoint-pollution model sensitivity to grid-cell size. *Journal of Water Resources Planning and Management*, *119*(2), 141–157.

WALTON, T.L., AND ADAMS, W.D., 1976. Capacity of inlet outer bars to store sand, American Society of Civil Engineers, 15th Coastal Engineering Conference, New York, Proceedings, p. 1919–1937. In: O'Connor, M. C., Cooper, J. A. G., & Jackson, D. W. T. (2011). Decadal Behavior of Tidal Inlet-Associated Beach Systems, Northwest Ireland, in Relation to Climate Forcing. *Journal of Sedimentary Research*, *81*(1), 38–51.

Wright, L. D. (1980). Beach cut in relation to surf zone morphodynamics. *Proc. 17th ICCE. ASCE, New York*, 978–996.

Wright, L. D., & Short, A. D. (1984). Morphodynamic variability of surf zones and beaches: a synthesis. *Marine Geology*, *56*(1-4), 93–118.

Yang, C.-S., Kao, S.-P., Lee, F.-B., & Hung, P.-S. (2004). Twelve Different Interpolation Methods: a Case Study of Surfer 8.0. *ISPRS*, 778–783.

Yılmaz, H. M. (2007). The effect of interpolation methods in surface definition : an experimental study. *Earth Surface Processes and Landforms*, *32*, 1346–1361.

SITES

http://www.csc.noaa.gov/magazine/2002/01/news.html (December, 2012)

http://www.oceanweather.com/research/HindcastApproach.html (January, 2013)

http://www.ecmwf.int/research/era/do/get/Re-analysis_ECMWF (January, 2014)

http://www.ecmwf.int/research/era (January, 2014)

http://www.ecmwf.int/en/research/modelling-and-prediction/marine (May, 2014)

APPENDIX

Python Script

```
# Tool Name: Beach Profile Graph (BeachProG)
# Author name: Ana Luísa Banja Martins
# email: albmartins.0306@gmail.com

#_____________________________________________________________________

# Import arcpy module
import arcpy
from arcpy.sa import *
from arcpy import env
import os
import sys

# Overwrite Output
arcpy.env.overwriteOutput = True

#_____________________________________________________________________
### Check for Extension
# Geostatistical Analyst
arcpy.CheckOutExtension('GeoStats')
#Spatial Analyst
arcpy.CheckOutExtension('Spatial')
# 3D Analyst
arcpy.CheckOutExtension('3D')

#_____________________________________________________________________
```

```
### Script arguments
in_data_points = arcpy.GetParameterAsText(0)
in_data_points_file = in_data_points.split(';')
Zvalue_field = arcpy.GetParameterAsText(1)
Output_cell_size = arcpy.GetParameterAsText(2)
StudyArea_polygon = arcpy.GetParameterAsText(3)
profile_line_location = arcpy.GetParameterAsText(4)
Profile_plane_height = arcpy.GetParameterAsText(5)
Plane_Height = arcpy.GetParameterAsText(6)
outputFolder = arcpy.GetParameterAsText(7)

#_____

#Get the path name to this script
scriptPath = sys.path[0]
#Get the pathname to the ToolShare folder
toolSharePath = os.path.dirname(scriptPath)
#Now construct pathname to the ToolData folder
toolDataPath = os.path.join(toolSharePath,"ToolData")
#Create the pathname to the graph template
templatePath = os.path.join(toolDataPath, "Template_graph.tee")
#Create the pathname to the graph series template
templategraphSeries = os.path.join(toolDataPath, "Template_graphSeries.tee")
arcpy.AddMessage("templatePath is " + templatePath)
#Now construct pathname to the RESULTS folder
```

```
toolResultsPath = os.path.join(toolSharePath,outputFolder)
arcpy.AddMessage("output folder " + toolResultsPath)
#Create the pathname to the raster symbology
RasterSymbologyPath = os.path.join(toolDataPath, "raster_symbology.lyr")
#Create the pathname to the minus raster symbology
MinusSymbologyPath = os.path.join(toolDataPath, "MINUS_symbology.lyr")

#_____________________________________________________________________

 ## shapefile name: ff_2004_02_10_prf
 ## split_data_points_name[0]=ff
 ## split_data_points_name[1]=2004
 ## split_data_points_name[2]=02
 ## split_data_points_name[3]=10
 ## split_data_points_name[4]=prf

#_____________________________________________________________________

env.workspace = toolResultsPath
i = 0
for in_data_points in in_data_points_file:
 arcpy.AddMessage("in_data is " + in_data_points)

 split_input_data_name = in_data_points.split('_')
 name = split_input_data_name[1] + split_input_data_name[2] +
split_input_data_name[3]
 arcpy.AddMessage("name is " + name)
```

Process: Create Radial Basis Function (Multiquadratic)

```
RBF = str('RB_') + name

featureClassName = arcpy.ValidateTableName(RBF, toolResultsPath)

outFeatureClass = os.path.join(toolResultsPath, featureClassName)

arcpy.RadialBasisFunctions_ga(in_data_points, Zvalue_field, '#', outFeatureClass,
Output_cell_size, 'NBRTYPE=Standard S_MAJOR=350 S_MINOR=200 ANGLE=355
NBR_MAX=16 NBR_MIN=5 SECTOR_TYPE=FOUR_SECTORS',
'MULTIQUADRIC_FUNCTION', '#') #'NBRTYPE=Standard S_MAJOR=350
S_MINOR=200 ANGLE=355 NBR_MAX=16 NBR_MIN=5
SECTOR_TYPE=FOUR_SECTORS'
```

Process: Extract by Mask (raster with study area)

```
rasterCLIPname = str('Cp_') + name

RC = arcpy.ValidateTableName(rasterCLIPname, toolResultsPath)

oRC = os.path.join(toolResultsPath, RC)

out_Extract_By_Mask = ExtractByMask(RBF, StudyArea_polygon)

out_Extract_By_Mask.save(oRC)
```

Process: Make Raster Layer

```
Raster_Layer_name = str('Rt_') + name

Raster_Layer = arcpy.MakeRasterLayer_management(oRC, Raster_Layer_name)
```

Process: Set the symbology of the output

```
RasterLayerWithSymbology =
arcpy.ApplySymbologyFromLayer_management(Raster_Layer, RasterSymbologyPath)
```

Process: Save to layer file

```
LYR_name = str('RBF_') + name
```

```
SAVELayer = os.path.splitext(LYR_name)[0] + ".LYR"

arcpy.SaveToLayerFile_management(RasterLayerWithSymbology, SAVELayer)
```

Process: Intersect (line with study area polygon)

```
lineCLIPname = 'LineClip'

LC = arcpy.ValidateTableName(lineCLIPname, toolResultsPath)

oLC = os.path.join(toolResultsPath, LC)

arcpy.Intersect_analysis ([profile_line_location, StudyArea_polygon], oLC, 'ALL', '#', 'INPUT')
```

Process: Extract by Mask (profile line)

```
extract_raster_by_line = str('L_') + name

EM = arcpy.ValidateTableName(extract_raster_by_line, toolResultsPath)

oEM = os.path.join(toolResultsPath, EM)

out_Extract_By_Mask_L = ExtractByMask(rasterCLIPname, 'LineClip.shp')

out_Extract_By_Mask_L.save(oEM)
```

Process: Raster to point

```
raster_cell_points = str('Points_') + name

SAVEraster_cell_to_points = os.path.splitext(raster_cell_points)[0] + ".SHP"

arcpy.RasterToPoint_conversion(extract_raster_by_line, SAVEraster_cell_to_points, 'Value')
```

Process: Feature Vertices To Points

```
fcList = arcpy.ListFeatureClasses('Line*')

for line in fcList:

vertice_name = "Vertice"
```

```
V = arcpy.ValidateTableName(vertice_name, toolResultsPath)

oV = os.path.join(toolResultsPath, V)

arcpy.FeatureVerticesToPoints_management(line, oV, 'START')


### Process: Point Distance

Distance_between_points = str('Dist_') + name

SAVEdistance_between_points = os.path.splitext(Distance_between_points)[0] +
".DBF"

arcpy.PointDistance_analysis('Vertice.shp', SAVEraster_cell_to_points,
SAVEdistance_between_points, '#')


### Process: Join field

arcpy.JoinField_management(SAVEraster_cell_to_points, 'FID',
SAVEdistance_between_points, 'NEAR_FID', '#')


### Process: Add XY

arcpy.AddXY_management(SAVEraster_cell_to_points)


### Process: Sort field

sort_field = str('Sort_') + name

SAVEsort_fields = os.path.splitext(sort_field)[0] + ".SHP"

arcpy.Sort_management(SAVEraster_cell_to_points, SAVEsort_fields, [['DISTANCE',
'ASCENDING']])


### Process: Add Field

arcpy.AddField_management(SAVEsort_fields, 'Z', 'DOUBLE', '10', '6', '#', '#',
'NON_NULLABLE', 'NON_REQUIRED', '#')
```

Process: Delete field

```
arcpy.DeleteField_management(SAVEsort_fields, ['INPUT_FID', 'NEAR_FID', 'POINTID', 'FREQUENCY'])
```

Process: Add Field

```
arcpy.AddField_management(SAVEsort_fields, 'AREA', 'DOUBLE', '10', '6', '#', '#', 'NON_NULLABLE', 'NON_REQUIRED', '#')
```

Process: Add Field

```
arcpy.AddField_management(SAVEsort_fields, 'Z_MIN', 'DOUBLE', '10', '6', '#', '#', 'NON_NULLABLE', 'NON_REQUIRED', '#')
```

Process: Calculate Z min

```
arcpy.CalculateField_management(SAVEsort_fields, 'Z_MIN', Profile_plane_height, 'PYTHON_9.3', '#')
```

Process: Calculate Z (= GRID_CODE + Zmin)

```
if Profile_plane_height < 0:


arcpy.CalculateField_management(SAVEsort_fields, 'Z', '!GRID_CODE! + abs(!Z_MIN!)', 'PYTHON_9.3', '#')

else:

arcpy.CalculateField_management(SAVEsort_fields, 'Z', '!GRID_CODE!', 'PYTHON_9.3', '#')
```

Process: New shapefile with Z value > Profile_plane_height

```
Name_new_sort_shapefile = str('shp_') + name

Save_Name_new_sort_shapefile = os.path.splitext(Name_new_sort_shapefile)[0] + ".SHP"
```

```
arcpy.Select_analysis(SAVEsort_fields,Save_Name_new_sort_shapefile,'"Z" >= "Z_MIN"')


### Process: Calculate Area
fc = Save_Name_new_sort_shapefile
H = []
CrossDist = []
area = []
cursor = arcpy.SearchCursor(fc, '', '')
for row in cursor:
H.append(row.Z)
CrossDist.append(row.DISTANCE)
for h in range (0,len(H)-1):
        h1=H[h]
        h2=H[h+1]
        cd1=CrossDist[h]
        cd2=CrossDist[h+1]
        if h1>h2:
                A=(h2*(cd2-cd1))+((0.5*(h1-h2))*(cd2-cd1))
        else:
                A=(h1*(cd2-cd1))+((0.5*(h2-h1))*(cd2-cd1))
        area.append(A)

del row, cursor
rows = arcpy.UpdateCursor(fc)
C = -1
```

```
for row in rows:
        row.setValue('AREA',area[C])
        C = C + 1
        rows.updateRow(row)
del row, rows
```

Process: Add Field

```
arcpy.AddField_management(Save_Name_new_sort_shapefile, 'A_TOTAL',
'DOUBLE', '10', '6', '#', '#', 'NON_NULLABLE', 'NON_REQUIRED', '#')
```

Process: Area TOTAL

```
fc = Save_Name_new_sort_shapefile
area_total = []
cursor = arcpy.SearchCursor(fc, '', '')
for row in cursor:
area_total.append(row.AREA)

del row, cursor
rows = arcpy.UpdateCursor(fc)
C = -1

for row in rows:
        row.setValue('A_TOTAL',sum(area_total))
        C = C + 1
        rows.updateRow(row)
del row, rows
```

Process: Minus

```
rasterList = arcpy.ListRasters('Cp*', 'GRID')
for rasterL in rasterList:
# Set local variables
if len(rasterList)>=2:

for R in range(0, len(rasterList)-1):
R1 = rasterList[R]
R2 = rasterList[R+1]
#Minus
Minus_name = str('M_') + name
RM = arcpy.ValidateTableName(Minus_name, toolResultsPath)
oRM = os.path.join(toolResultsPath, RM)

arcpy.Minus_3d(R1, R2, oRM)
```

Process: Make Raster Layer

```
min_Layer_name = str('MINlyr_') + name
min_Layer = arcpy.MakeRasterLayer_management(oRM, min_Layer_name)
```

Process: Set the symbology of the output

```
MinLayerWithSymbology =
arcpy.ApplySymbologyFromLayer_management(min_Layer, MinusSymbologyPath)
```

Process: Save to layer file

```
SAVE_MIN_layer = os.path.splitext(min_Layer_name)[0] + ".LYR"
arcpy.SaveToLayerFile_management(MinLayerWithSymbology, SAVE_MIN_layer)
```

Process: surface volume

```
surface_volume = 'Total_Volume'

save_surface_volume = os.path.splitext(surface_volume)[0] + ".CSV"

arcpy.SurfaceVolume_3d(oRC,save_surface_volume,"ABOVE",Plane_Height,"1","0")
```

Process: surface volume from MINUS rasters

```
# surface_volume_minus = 'Total_Volume_Minus'

# save_surface_volume_minus = os.path.splitext(surface_volume_minus)[0] + ".CSV"

# rasterList_minus = arcpy.ListRasters('M_*', 'GRID')

# for rasterMinus in rasterList_minus:

# arcpy.SurfaceVolume_3d(rasterMinus, save_surface_volume_minus, 'ABOVE',
Plane_Height, '1', '0')
```

Process: Input surface information

```
arcpy.AddSurfaceInformation_3d('LineClip.shp',oRC,"AVG_SLOPE","BILINEAR","#
","1","0")
```

Process: Join Avg_Slope to shapefile

```
arcpy.JoinField_management(Save_Name_new_sort_shapefile,"FID","LineClip.shp","F
ID","Avg_Slope")
```

Process: Make graph

```
# Set local variables

graph_name = str('GRF_') + name

outMakegraph_IMG = os.path.splitext(graph_name)[0] + ".JPG"
```

```
# Create the graph
graph = arcpy.Graph()
# Add a vertical line series to the graph
graph.addSeriesLineVertical(SAVEsort_fields, 'GRID_CODE', 'DISTANCE')
# Specify the title of the left axis
graph.graphAxis[0] = "Elevation"
# Specify the title of the bottom axis
graph.graphAxis[2] = "Cross-Distance"
# Specify the subtitle of the graph
graph.graphPropsGeneral.subtitle = name
# Output a graph, which is created in-memory
arcpy.MakeGraph_management(templatePath, graph, graph_name)
# Save the graph as an image
arcpy.SaveGraph_management(graph_name, outMakegraph_IMG,
"MAINTAIN_ASPECT_RATIO", "600", "375")


### Process: Make graph Series
List_feature = arcpy.ListFeatureClasses('Sort_*')
for series in range(0, len(List_feature)-1):


first_profile = List_feature[0]
second_profile = List_feature[-1]


# Set local variables
graphSeries_name = "Profile Graph"
outMakegraphSeries_IMG = os.path.splitext(graphSeries_name)[0] + ".JPG"
# Create the graph
```

```
graphseries = arcpy.Graph()
# Add a vertical line series to the graph
graphseries.addSeriesLineVertical(first_profile, 'GRID_CODE', 'DISTANCE')
graphseries.addSeriesLineVertical(second_profile, 'GRID_CODE', 'DISTANCE')
# Specify the subtitle of the graph
first_profile_split = first_profile.split('_')
second_profile_split = second_profile.split('_')
first_profile_name = first_profile_split[1]
second_profile_name = second_profile_split[1]

first_BPG = first_profile_name.split('.')
second_BPG = second_profile_name.split('.')
first_BPG_name = first_BPG[0]
second_BPG_name = second_BPG[0]
graphseries.graphPropsGeneral.subtitle = first_BPG_name + ', ' + second_BPG_name
# Output a graph, which is created in-memory
arcpy.MakeGraph_management(templategraphSeries, graphseries, graphSeries_name)
# Save the graph as an image
arcpy.SaveGraph_management(graphSeries_name, outMakegraphSeries_IMG,
"MAINTAIN_ASPECT_RATIO", "600", "375")

#_____________________________________________________________

### Process: Convert table to excel. ONLY FOR ARCGIS 10.2!!!!!!!!!
TableToExcelname = name
outTableToTable = os.path.splitext(TableToExcelname)[0] + ".xls"
```

```
 arcpy.TableToExcel_conversion(Save_Name_new_sort_shapefile,
outTableToTable,"ALIAS","CODE")

#_____________________________________________________________________

# Process: Delete data from disk

arcpy.Delete_management(outFeatureClass)

arcpy.Delete_management('LineClip.shp')

arcpy.Delete_management(oEM)

arcpy.Delete_management(SAVEraster_cell_to_points)

arcpy.Delete_management('Vertice.shp')

arcpy.Delete_management(SAVEdistance_between_points)

#arcpy.Delete_management(SAVEsort_fields)



i = i + 1
```